This paper is published as part of a PCCP Themed Issue on:
Coarse-grained modeling of soft condensed matter

Guest Editor: Roland Faller (UC Davis)

Editorial

Coarse-grained modeling of soft condensed matter
Phys. Chem. Chem. Phys., 2009 **DOI:** 10.1039/b903229c

Perspective

Multiscale modeling of emergent materials: biological and soft matter
Teemu Murtola, Alex Bunker, Ilpo Vattulainen, Markus Deserno and Mikko Karttunen, *Phys. Chem. Chem. Phys.*, 2009 **DOI:** 10.1039/b818051b

Communication

Dissipative particle dynamics simulation of quaternary bolaamphiphiles: multi-colour tiling in hexagonal columnar phases
Martin A. Bates and Martin Walker, *Phys. Chem. Chem. Phys.*, 2009 **DOI:** 10.1039/b818926a

Papers

Effective control of the transport coefficients of a coarse-grained liquid and polymer models using the dissipative particle dynamics and Lowe–Andersen equations of motion
Hu-Jun Qian, Chee Chin Liew and Florian Müller-Plathe, *Phys. Chem. Chem. Phys.*, 2009
DOI: 10.1039/b817584e

Adsorption of peptides (A3, Flg, Pd2, Pd4) on gold and palladium surfaces by a coarse-grained Monte Carlo simulation
R. B. Pandey, Hendrik Heinz, Jie Feng, Barry L. Farmer, Joseph M. Slocik, Lawrence F. Drummy and Rajesh R. Naik, *Phys. Chem. Chem. Phys.*, 2009 **DOI:** 10.1039/b816187a

A coarse-graining procedure for polymer melts applied to 1,4-polybutadiene
T. Strauch, L. Yelash and W. Paul, *Phys. Chem. Chem. Phys.*, 2009 **DOI:** 10.1039/b818271j

Anomalous waterlike behavior in spherically-symmetric water models optimized with the relative entropy
Aviel Chaimovich and M. Scott Shell, *Phys. Chem. Chem. Phys.*, 2009 **DOI:** 10.1039/b818512c

Coarse-graining dipolar interactions in simple fluids and polymer solutions: Monte Carlo studies of the phase behavior
B. M. Mognetti, P. Virnau, L. Yelash, W. Paul, K. Binder, M. Müller and L. G. MacDowell, *Phys. Chem. Chem. Phys.*, 2009 **DOI:** 10.1039/b818020m

Beyond amphiphiles: coarse-grained simulations of star-polyphile liquid crystalline assemblies
Jacob Judas Kain Kirkensgaard and Stephen Hyde, *Phys. Chem. Chem. Phys.*, 2009 **DOI:** 10.1039/b818032f

Salt exclusion in charged porous media: a coarse-graining strategy in the case of montmorillonite clays
Marie Jardat, Jean-François Dufrêche, Virginie Marry, Benjamin Rotenberg and Pierre Turq, *Phys. Chem. Chem. Phys.*, 2009 **DOI:** 10.1039/b818055e

Improved simulations of lattice peptide adsorption
Adam D. Swetnam and Michael P. Allen, *Phys. Chem. Chem. Phys.*, 2009 **DOI:** 10.1039/b818067a

Curvature effects on lipid packing and dynamics in liposomes revealed by coarse grained molecular dynamics simulations
H. Jelger Risselada and Siewert J. Marrink, *Phys. Chem. Chem. Phys.*, 2009 **DOI:** 10.1039/b818782g

Self-assembling dipeptides: conformational sampling in solvent-free coarse-grained simulation
Alessandra Villa, Christine Peter and Nico F. A. van der Vegt, *Phys. Chem. Chem. Phys.*, 2009 **DOI:** 10.1039/b818144f

Self-assembling dipeptides: including solvent degrees of freedom in a coarse-grained model
Alessandra Villa, Nico F. A. van der Vegt and Christine Peter, *Phys. Chem. Chem. Phys.*, 2009 **DOI:** 10.1039/b818146m

Computing free energies of interfaces in self-assembling systems
Marcus Müller, Kostas Ch. Daoulas and Yuki Norizoe, *Phys. Chem. Chem. Phys.*, 2009 **DOI:** 10.1039/b818111j

Anomalous ductility in thermoset/thermoplastic polymer alloys
Debashish Mukherji and Cameron F. Abrams, *Phys. Chem. Chem. Phys.*, 2009 **DOI:** 10.1039/b818039c

A coarse-grained simulation study of mesophase formation in a series of rod–coil multiblock copolymers
Juho S. Lintuvuori and Mark R. Wilson, *Phys. Chem. Chem. Phys.*, 2009 **DOI:** 10.1039/b818616b

Simulations of rigid bodies in an angle-axis framework
Dwaipayan Chakrabarti and David J. Wales, *Phys. Chem. Chem. Phys.*, 2009 **DOI:** 10.1039/b818054g

Effective force coarse-graining
Yanting Wang, W. G. Noid, Pu Liu and Gregory A. Voth, *Phys. Chem. Chem. Phys.*, 2009 **DOI:** 10.1039/b819182d

Backmapping coarse-grained polymer models under sheared nonequilibrium conditions
Xiaoyu Chen, Paola Carbone, Giuseppe Santangelo, Andrea Di Matteo, Giuseppe Milano and Florian Müller-Plathe, *Phys. Chem. Chem. Phys.*, 2009 **DOI:** 10.1039/b817895j

Energy landscapes for shells assembled from pentagonal and hexagonal pyramids
Szilard N. Fejer, Tim R. James, Javier Hernández-Rojas and David J. Wales, *Phys. Chem. Chem. Phys.*, 2009
DOI: 10.1039/b818062h

Molecular structure and phase behaviour of hairy-rod polymers
David L. Cheung and Alessandro Troisi, *Phys. Chem. Chem. Phys.*, 2009 **DOI:** 10.1039/b818428c

Molecular dynamics study of the effect of cholesterol on the properties of lipid monolayers at low surface tensions
Cameron Laing, Svetlana Baoukina and D. Peter Tieleman, *Phys. Chem. Chem. Phys.*, 2009 **DOI:** 10.1039/b819767a

On using a too large integration time step in molecular dynamics simulations of coarse-grained molecular models
Moritz Winger, Daniel Trzesniak, Riccardo Baron and Wilfred F. van Gunsteren, *Phys. Chem. Chem. Phys.*, 2009 **DOI:** 10.1039/b818713d

The influence of polymer architecture on the assembly of poly(ethylene oxide) grafted C_{60} fullerene clusters in aqueous solution: a molecular dynamics simulation study
Justin B. Hooper, Dmitry Bedrov and Grant D. Smith, *Phys. Chem. Chem. Phys.*, 2009 **DOI:** 10.1039/b818971d

Determination of pair-wise inter-residue interaction forces from folding pathways and their implementation in coarse-grained folding prediction
Sefer Baday, Burak Erman and Yaman Arkun, *Phys. Chem. Chem. Phys.*, 2009 **DOI:** 10.1039/b820801h

Multiscale modeling of emergent materials: biological and soft matter

Teemu Murtola,[a] Alex Bunker,[bc] Ilpo Vattulainen,[ade] Markus Deserno[f] and Mikko Karttunen*[g]

Received 14th October 2008, Accepted 12th February 2009
First published as an Advance Article on the web 25th February 2009
DOI: 10.1039/b818051b

In this review, we focus on four current related issues in multiscale modeling of soft and biological matter. First, we discuss how to use structural information from detailed models (or experiments) to construct coarse-grained ones in a hierarchical and systematic way. This is discussed in the context of the so-called Henderson theorem and the inverse Monte Carlo method of Lyubartsev and Laaksonen. In the second part, we take a different look at coarse graining by analyzing conformations of molecules. This is done by the application of self-organizing maps, *i.e.*, a neural network type approach. Such an approach can be used to guide the selection of the relevant degrees of freedom. Then, we discuss technical issues related to the popular dissipative particle dynamics (DPD) method. Importantly, the potentials derived using the inverse Monte Carlo method can be used together with the DPD thermostat. In the final part we focus on solvent-free modeling which offers a different route to coarse graining by integrating out the degrees of freedom associated with solvent.

I. Introduction

A Emergent properties

In biological and soft matter systems a broad spectrum of modes of motion, operating over an immense range of length and time scales, are simultaneously active at ambient temperature. These modes can not be trivially uncoupled, resulting in multiscale behaviour: the systems self-organize and express what can be referred to as "emergent properties". What is referred to as "Life" is a subset of these materials; the importance of understanding the physics in biological systems may be summarized by the famous quote from Richard Feynman[1]

"Certainly no subject or field is making more progress on so many fronts at the present moment than biology, and if we were to name the most powerful assumption of all, which leads one on and on in an attempt to understand life, it is that all things are made of atoms, and that everything that living things do can be understood in terms of the jigglings and wigglings of atoms."

No biological phenomenon has been encountered whose compliance with the laws of physics has been seriously challenged.

[a] *Department of Applied Physics and Helsinki Institute of Physics, Helsinki University of Technology, Finland*
[b] *Centre for Drug Research, Faculty of Pharmacy, University of Helsinki, Finland*
[c] *Laboratory of Physical Chemistry and Electrochemistry, Helsinki University of Technology, Finland*
[d] *MEMPHYS—Center for Biomembrane Physics, Physics Department, University of Southern Denmark, Odense, Denmark*
[e] *Department of Physics, Tampere University of Technology, Finland*
[f] *Department of Physics, Carnegie Mellon University, 5000 Forbes Ave., Pittsburgh, PA 15213, USA*
[g] *Department of Applied Mathematics, The University of Western Ontario, London, Ontario, Canada. E-mail: mkarttu@uwo.cawww.softsimu.org*

Teemu Murtola

Teemu Murtola is currently a PhD student at the Department of Applied Physics at the Helsinki University of Technology, Finland. His thesis, supervised by Prof. Ilpo Vattulainen, focuses on the use of structural information from detailed simulations in constructing coarse-grained models.

Alex Bunker

Alex Bunker currently has a joint position in the Faculty of Pharmacy at the University of Helsinki and the Department of Chemistry at the Helsinki University of Technology. He obtained his PhD in physics from the University of Georgia in 1998, and has subsequently worked at the Max Planck Institute for Polymer Research and Unilever R&D Port Sunlight. His expertise is in the use of Monte Carlo, molecular dynamics and dissipative particle dynamics simulation techniques, the hybridization of these methods and their application to a wide range of problems in material science, soft matter physics, colloid chemistry and biological physics.

This review outlines some of the recent developments in modeling techniques capable of simultaneously studying multiple length and time scales, collectively referred to as "multiscale modeling", that make theoretical understanding of these emergent materials possible. Their multiscale nature is best illustrated through examples.

1 Example: different scales in biological systems. Water is the most common and crucial element in all biological systems.[2] A water molecule is approximately 10^{-10} m in size, and the relevant time scale is defined by molecular vibrations which occur at times of the order of 10^{-15} s. The biologically important problem of protein folding, however, can take anything from 1 μs up to about 1000 s depending on the size of the protein.[3] This huge spread in time scales is due to the fact that proteins express a hierarchy of spatial ordering, *i.e.*, primary, secondary and tertiary structure, see *e.g.* ref. 4, on different interdependent scales. Proteins may, and often do, form complexes with other proteins, the complexes of several proteins acting as biological machines performing functions as intricate as moving flagella to propel cells. Finally, from a cell's point of view, the largest time scale corresponds to the lifetime of a cell, which is usually of the order of months.

Double stranded (ds) DNA can often be viewed as a relatively stiff polymer with a persistence length of about 50 nm. The total length of all dsDNA in every (diploid) human cell is about 2 meters, distributed over 23 pairs of chromosomes, and it is hierarchically compacted inside the cell nucleus through an incredibly elaborate self-organized structure with specially designed protein complexes composed of elements on many length scales: 8 proteins form a disc shaped nucleosome around which the dsDNA is wound $1\frac{2}{3}$ times. The whole complex has a thickness of 6 nm and a diameter of 10 nm. These nucleosomes in turn self assemble into chromatin fibres, tubes with a diameter of 30 nm, which are wound to form the four lobed structure of the chromosomes. Not only is this structure complex, with elements on many length scales, but within the intricacies of its structure are elements primed to trigger exact subsets to unwind for expression.[5–7]

Protein complexes and DNA operate with a variety of other metabolically important molecules in a water solvent encapsulated in a phospholipid membrane that forms a cell, typically with a size of approximately 10 μm. All components of the cell interact in an interplay of feedback upon feedback, ultimately setting up a flow of free energy that creates order inside the cells—this is the essence of cell metabolism (see *e.g.*, ref. 8).

2 Example: different scales in polymers and colloids. Biological systems can be seen as combinations of two types of molecular structures: colloids and polymers. It is really the field of polymers where the ideas of linking many time and length scales have developed the fastest. This is easy to understand through the following simple example: the time scales associated with bond vibrations are roughly 10^{-15} s while conformational transitions associated with individual bonds occur typically in time scales of 10^{-11} s. The related

Ilpo Vattulainen

Ilpo Vattulainen is a professor of biological physics at Tampere University of Technology in Finland leading a team of about 25 people. His group is affiliated to two centres of excellence, one in the Helsinki University of Technology and another in the University of Southern Denmark. The group focuses on computational and theoretical studies of biomembranes, membrane proteins, drugs, sterols, carbohydrates, nanomaterials, lipoproteins and the related processes and phenomena associated with these systems. During his free time, he travels by train between Tampere and Helsinki.

Markus Deserno

Markus Deserno studied physics at the universities Erlangen/Nuremberg (Germany) and York (GB). In his PhD work at the Max Planck Institute for Polymer Research (MPI-P) in Mainz (Germany) he studied counterion condensation for rigid linear polyelectrolytes using theory and simulation. During a postdoctoral stay at the department of chemistry and biochemistry at UCLA he began to focus on lipid membrane biophysics. He returned to the MPI-P and led a research group dedicated to studying the biophysics of mesoscopic membrane processes using continuum theory and coarse-grained simulation. He is currently associate professor of physics at Carnegie Mellon University.

Mikko Karttunen

Mikko Karttunen studied physics at Tampere University of Technology, Finland. His PhD at the Dept. of Physics at McGill University in Montreal focused on driven charge-density waves and superconductors. He shifted his focus toward soft matter and biological systems during his postdoctoral stay at the Max Planck Institute for Polymer Research in Mainz and while working as an Academy of Finland Fellow in Helsinki University of Technology. He is currently an Associate Professor of Applied Mathematics at the University of Western Ontario in London, Canada, leading a group of about 10 people. In his free time he enjoys running and cooking.

changes taking place along the chain take orders of magnitude longer than these time scales. Furthermore, processes such as spinodal decomposition, or phase separation in general, have characteristic times of at least seconds.

The intricate multiscale structures of colloids result from the extremely complex interplay of different competing enthalpic and entropic intermolecular forces, some short range such as van der Waals and steric forces operating on the length scale of Ångstroms, and some long range including electrostatic interactions and entropic effective forces which operate over much longer length scales. For example, the Coulomb interaction behaves as $1/r$ (in 3D), which makes it long-ranged. Screening of interactions and correlations typically complicate matters for both electrostatic and hydrodynamic interactions.

The interacting structural units of colloid materials can be very large, in the range 500 nm–10 μm, for example. All of these factors result in a material whose macroscopic properties can be altered dramatically through very subtle changes in their ingredients. In some cases, adding trace amounts, as little as a few mole percent, can induce a transformation from a thin liquid to the consistency of butter. For example, the problem of creating household cleaners that appear "thick" and thus effective, but still pour and spread, at minimal amount of (expensive) surfactant added to (cheap) water is of great interest to colloid scientists working in the home and personal care industry. As a result of this flexibility, colloid science has a very broad range of applications from food science and cosmetics to materials science and chemical and biomedical engineering. In addition to the complete range of length scales, colloids exhibit dynamics and structural changes of the full range of time scales, from interatomic vibrations on the scale of femtoseconds to gelation and separation that can occur on the time scale of days to weeks.

B Principles of molecular modeling

While the computational approach has in the past met with some degree of skepticism, today, there is no doubt about the value of computer simulations; advances in theory, experiments, and computational modeling go hand in hand. This is particularly so in interdisciplinary fields such as soft matter and biophysics.[9–12] In a nutshell, computer simulations allow us to do theoretical experiments under perfectly controlled approximations, thus providing a bridge between theory and experiments. Indeed, molecular modeling has been aptly described as "the science and art of studying molecular structure and function through model building and computation".[13]

Constructing a model is a process independent from the use of any computational methods but is the key central element upon which any computational simulation is based. The structure of DNA, for example, was first discovered using this approach, using an actual physical model (on display at the Science Museum of London) assembled out of clamps and stands from the chemistry lab. The discovery of C_{60} buckminsterfullerene provides another example, as the first prototype of its structure created by Richard E. Smalley was made of paper sheets.[14]

For a model to be used in a computer simulation, the starting point of building the model is the topology and initial structures of molecules that typically need input from experiments such as nuclear magnetic resonance (NMR), various scattering, and spectroscopic techniques. Having done this, one needs to write down the Hamiltonian operator, $\mathscr{H}$, that includes all interactions present in the model system. Then, the "force field", *i.e.*, all the physical parameters of the Hamiltonian operator (in classical simulations), is constructed.

Finally, all molecular systems are embedded in a thermal environment that dictates their thermodynamic properties. While the pathway from a Hamiltonian to a free energy is perfectly clear, the necessary computation of the partition function is essentially always technically impossible. Computers have become an invaluable tool to arrive at equilibrated thermal properties by cleverly sampling the phase space of the system using a variety of tricks that have been well documented elsewhere, see *e.g.* ref. 15–17. Of course, not all important questions are related to static thermal equilibrium, but even this seemingly simplest of all problems generally requires a massive investment of intelligent computing, and it warns us how much more complicated other tasks (nonequilibrium, kinetics, rare events, *etc.*) are likely going to be.

C Multiscale modeling

There exists a large number of different computational methods for modeling materials, each optimal for addressing a different length/time scale. Starting at the bottom, *ab initio* simulations take quantum mechanical details of electron orbital structure into account, limiting the obtainable system sizes to a few hundred atoms. This is because for these methods the required computational effort scales very unfavorably with the number of particles. For example a commonly used approach, density functional theory, scales as $O(N^3)$[21,22] while classical molecular dynamics scales as $O(N)$.

Consequently, quantum mechanical approaches are appropriate for issues where electronic degrees of freedom cannot be neglected. In the context of coarse graining, they can be used to develop force fields for classical molecular dynamics (MD) simulations which are able to reach time scales of the order of 100 ns, and linear system sizes of some tens of nanometers, see *e.g.* Niemelä *et al.*[23]

Despite this massive increase in tractable system size, many questions of practical importance involve system sizes and time scales that significantly exceed what can be treated in classical atomistic simulations—not just now, but for many years to come. The time scales are the main obstacle. Unlike individual chemical bonds, larger aggregates of matter are not necessarily stiff. The implied weak forces that restore any perturbation away from equilibrium thus imply long equilibration times. Moreover, the complex modes of relaxation typically scale again very unfavorably with system size, such that looking at seemingly slightly enlarged length scales forces one to invest orders of magnitude more computation time just to equilibrate the system, because the dynamical time-range has increased so much.

The solution to this problem lies in continuing the process that we have begun when we developed force fields for use in

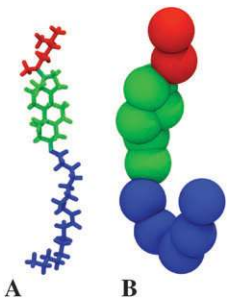

Fig. 1 A detailed atomistic and a coarse-grained model, using the MARTINI[18–20] model, of a cholesteryl oleate molecule. Different moieties are marked in red (short polar moiety), green (sterol ring), and blue (oleate chain).

classical molecular dynamics (MD) simulations using the results of the quantum mechanical calculation. The results of the classical MD calculation can in turn be used to create parameters for a new simulation capable of exploring length and time scales of yet-greater orders of magnitude, an example of this is the simulation of viral capsids by Arkhipov *et al.*[24] Theoretically this process can be continued indefinitely and is commonly referred to as coarse graining, Fig. 1 and 2 show examples of a coarse-grained lipid and high density lipoprotein particles, colloquially referred to as 'good cholesterol'. A theoretically inclined physicist will recognize the ideas of renormalization group (RG) theory at work, see *e.g.* ref. 25. Indeed, the process of systematic coarse graining requires "integrating out" degrees of freedom and arriving, on a larger scale, at effective degrees of freedom between which renormalized interactions operate. Just as in RG, this "integrating out" is the difficult component, but this is exactly where the power of simulations to create equilibrated ensembles comes in so usefully.

We thus have established the concept called multiscale modeling: a linked hierarchy of different methods, each being valid and useful over a certain well-defined length and time scale used together to gain mechanistic insight into the structure and dynamics of materials. Multiscale modeling has recently attracted a rapidly increasing amount of attention in computational materials research. There are a large number of reviews and books regarding soft and biological matter of which the most recent ones with a focus on coarse graining are, to our knowledge, ref. 26–31.

The multiscale approach, as we have just described it, sounds like a universal algorithm, capable of simulating any material regardless of complexity on all length scales simultaneously, capable of rendering the scientist who runs and analyzes the simulation results omnipotent regarding all aspects of the system's function. This of course sounds far too good to be true and it is, as within the heart of the approach lies a fundamental problem: while multiscaling is a universal idea, there is no ready-to-use algorithm appropriate for every conceivable situation. In other words, there is no unique way to perform coarse graining.

In addition to coarse-graining, multiscale modeling involves a second process: fine graining. Coarse graining, the transformation of detailed models to simplified descriptions with less degrees of freedom, effectively averages over some chosen properties of microscopic entities to form larger basic units. In fine graining, the opposite is achieved as one maps a coarser model to a more detailed one where configurational properties are generally the key quantities. A typical application of fine graining would be this: after one has successfully equilibrated a complicated system by using a coarse-grained model, thus relaxing the soft modes (which live on large length and time-scales), one would like to re-introduce the original detail, for instance in order to learn how the structure of the equilibrated large-scale matrix affects the local chemistry.

D Beyond molecules

The above discussion focused on molecular properties as coarse-graining molecular systems is the main theme of this review. Let us, for completeness, briefly discuss modelling of biologically motivated systems beyond molecules.

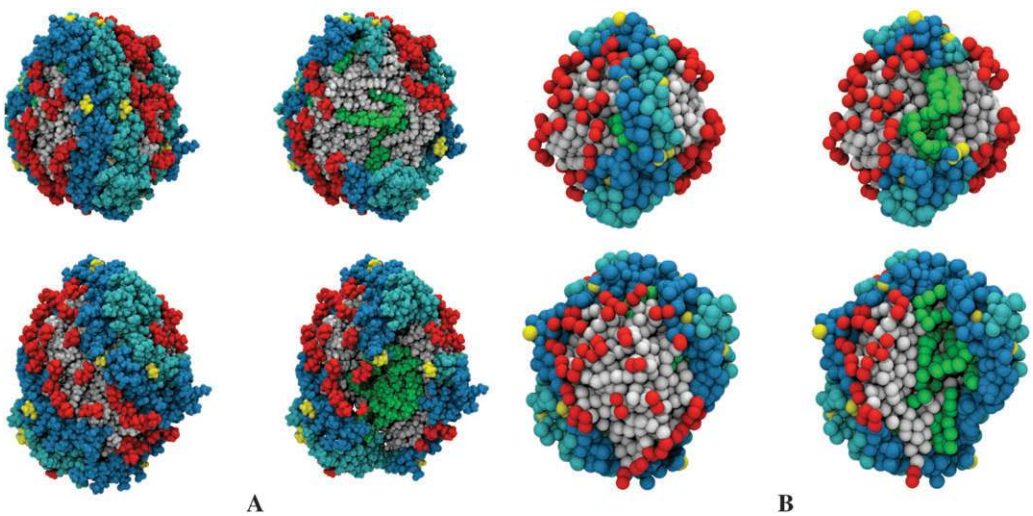

Fig. 2 Modeling high density lipoprotein (HDL) particles using detailed atomistic approach and coarse-grained MARTINI[18–20] model. The first snapshots (A) show the atomistic model and the other four (B) the coarse-grained model (Figure courtesy of Andrea Catte). Coarse graining and remodeling of a HDL system is discussed in detail by Catte *et al.*[32] Fig. 1 shows the coarse graining used for cholesterol molecules.

On the analytical side, methods based on the projection operator formalism of Mori and Zwanzig[33,34] have recently emerged through works of several groups, including the works by Akkermans and Briels,[35] the so-called GENERIC approach[36–38] of Öttinger *et al.*, and Majaniemi and Grant.[39] Ideally, the operator formalism offers a more rigorous and systematic approach.

Integral equations,[40] often viewed as a combination of the Ornstein–Zernike equation with some closure relation, offer another approach. The hypernetted chain (HNC) closure is a particularly popular choice in soft matter systems[41,42] and coarse graining.[43–45] At best, this approach can yield very accurate results,[46] but the analytical or numerical treatment gets complicated very quickly. It is important to notice that the HNC theory does not provide an exact solution since it uses an approximative closure relation. Integral equations have achieved a very high level of sophistication and constitute a field of research on their own right, and we refer the reader to the above references and references therein.

Other coarse-grained approaches which are more focused on hydrodynamics include the lattice Boltzmann method[47] and the stochastic rotation method (also referred to as 'multiparticle collision dynamics' or the 'Malevanets–Kapral method') developed by Malevanets and Kapral.[48,49] It couples a molecular level description with a mesoscale treatment of solvent conserving hydrodynamics. Malevanets and Yeomans have further developed a variant of the stochastic rotation dynamics method and applied that to study structural and dynamical properties of individual polymer chains in a hydrodynamic medium.[50,51] Recent developments of the technique are discussed in ref. 52–57. Yet another new approach is Green's function-based molecular dynamics (GFMD) simulations.[58] Thus far the method has been applied to contact mechanics and it remains to be seen how it can applied to soft elastic manifolds.

In the context of membranes, elastic continuum theories have been very successful as evidenced by a very rich literature starting with the seminal works of Canham,[59] Evans[60] and in particular Helfrich.[61] Here, membranes are described as two-dimensional fluid surfaces with an energy density that can be expanded in local geometric invariants—the curvature terms being of particular significance.

In recent years approaches using finite element methods[62] have also gained popularity in modeling biological and soft matter. The most recent models in 2D[63] and with full 3D elasticity[64–66] have been introduced to explain the behaviours of cytoskeletal networks with and without molecular motors, such as myosin. These models do not link directly to molecular properties but use time- and length scales, elastic constants and frequencies. There are, however, on-going attempts to combine the molecular level approach with these finite-element-like models.

The methods we have discussed so far span from classical MD to coarse-grained techniques. There has also been a great amount of activity in coupling quantum mechanical and classical MD level models. We refer the reader to the article by Kalibaeva and Ciccotti in ref. 26 for an in-depth discussion.

Algorithmic developments are an equally important issue, and we refer the reader to recent textbooks in the field, such as the ones by Leach[17] and Frenkel and Smit.[15]

E Routes to coarse graining

The methods that have been developed to achieve coarse-grained descriptions of physical systems in general—and soft materials in particular—can be roughly divided into five categories:

1. Phenomenological methods such as dissipative particle dynamics or Ginzburg–Landau type approaches
2. Analytical approaches based on the operator projection formalism
3. Construction of coarse-grained potentials by matching structure or forces between the two tiers of resolution
4. The analysis of the occurrence rates of different processes
5. Techniques such as self-organizing maps to coarse-grain molecular representations

Some approaches for selecting the coarse-grained degrees of freedom have already been proposed. Some of these methods are based on the analysis of a single structure, either using rigidity[67] or topology[68] to define the interacting units. Another class of methods uses dynamic information from the detailed model, either in the form of normal modes[69] or representing the detailed model as a complex network.[70] Here, we discuss a somewhat different approach based on analysis of the conformations produced by the simulation.

F Summary of article structure

In this article we will begin, in the following section, with a general discussion of the relevant issues pertaining to coarse graining, the Henderson theorem, and the inverse Monte Carlo method to obtain coarse-grained potentials. This will be followed by a detailed treatment of a particularly promising new method to aid the selection of good coarse-grained degrees of freedom: the use of self-organizing maps in section III. In section IV we will present an overview of a method for solving the dynamical equations of motion for coarse-grained systems: dissipative particle dynamics (DPD). In section V we discuss the next step in coarse graining: the removal of the physically often-uninteresting solvent and replacement with implicit functions.

The above seemingly different methods are directly related to each other: self-organizing maps can be used to select the relevant degrees of freedom, inverse Monte Carlo can be, and has been, used to obtain coarse-grained potentials from atomistic simulations, and those potentials have been used together with the DPD thermostat. Finally, solvent-free modeling offers a step towards even longer time and length scales and a possibility to study structures in even larger systems.

II. Using structural information: iterative methods and density functional theory

In the introduction, we discussed multiscale modeling in terms of coarse graining and fine graining. One possible method to generate the pairwise potentials at the coarse-grained level, *i.e.* perform coarse graining, is to first obtain them through phenomenological means, then justify them *a posteriori*. This is the method used, for example, in the case of DPD or the MARTINI model.[18–20] It is, however, also possible to derive the interaction potentials in a systematic fashion, and this is

what we will be discussing in the this section. Several of the methods that achieve this rely on what is known as the Henderson theorem, to be derived in section IIA.

One of the original tasks that integral equations were designed for is the estimation of pair correlation functions, $g(r)$, given the interaction potentials between the particles in the system, in the simplest case the particle particle pair potentials, $U(r)$. A key step to achieve coarse graining is performing essentially the inverse of this calculation. Performing an MD simulation on the fine grained model of the system gives us a result for the effective pair correlation function for the coarse-grained particles. This result must then be used to determine the interaction potentials between the coarse-grained particles. This problem has received considerable attention: which interaction potential would give rise to a pair-correlation function that matches the pair correlations in a fine grained system? While this inverse calculation is clearly far more complex than the original, there exists a far more fundamental problem: does a unique solution even exist?

The theoretical basis on which one could begin to contemplate this problem was given by Henderson,[71] who proved that under rather weak conditions two pair potentials which give rise to the same $g(r)$ cannot differ by more than a constant. This constant itself is not of great significance and can be fixed by the condition $V(r \to \infty) \to 0$, where r is the interparticle distance. A proof that such a pair potential always exists, again under rather weak conditions, has been given by Chayes *et al.*[72,73]

This approach is analogous to the Hohenberg–Kohn theorem[74] which states that all ground state properties are determined by the electron density, in the sense that a unique functional exists which can represent them exactly. This theorem is one of the cornerstones of modern density functional theory.

It is important to notice that the RDF obtained from a simulation includes effects from the many-body interactions. Furthermore, in this way it is possible to define new interaction sites and to compute the RDF between them, and thus readily obtain new coarse-grained models at different levels of description.

A Henderson theorem—relation to density functional theory

The Henderson theorem, powerful as it is, is remarkably simple to prove. Let us summarize here the essence of the argument. Uniqueness of the potential follows as a beautiful application of the Gibbs–Bogoliubov inequality (also referred to as Gibbs–Bogoliubov–Feynman or Feynman–Kleinert variational principle[75] depending on the context). For two systems with Hamiltonians H_1 and H_2 the following inequality holds for their free energies:

$$F_1 \leq F_2 + \langle H_2 - H_1 \rangle_1, \tag{2.1}$$

where $\langle \cdots \rangle_1$ denotes the (canonical) average appropriate for H_1. The key point is that equality holds if, and only if, $H_1 - H_2$ is independent of all degrees of freedom, which implies that the pair potentials can differ only by a constant. Consider now two systems which are identical in all respects except that the pair potential in one is u_1 and the pair potential in the other is u_2. The corresponding two particle distributions are g_1 and g_2. The uniqueness theorem asserts that if $g_1 \equiv g_2$ then $u_1 - u_2$ is a constant. Now, if u_1 and u_2 differ by more than just a constant, the same holds for H_1 and H_2, and thus equality in eqn (2.1) cannot hold, *i.e.*, we have $F_1 < F_2 + \langle H_2 - H_1 \rangle_1$, or more explicitly

$$f_1 < f_2 + \tfrac{1}{2} n \int \mathrm{d}^3 r [u_2(r) - u_1(r)] g_1(r). \tag{2.2}$$

where the f_i are the free energies per particle and n is the average particle density. The clue is that the above argument can be repeated with system 1 and 2 interchanged, which leads to

$$f_2 < f_1 + \tfrac{1}{2} n \int \mathrm{d}^3 r [u_1(r) - u_2(r)] g_2(r). \tag{2.3}$$

If we now use the fact that $g_1 \equiv g_2$ and add the inequalities (2.2) and (2.3), we obtain the contradiction $0 < 0$. This proves that the initial assumption that u_1 and u_2 differ by more than a constant must be wrong.

Uniqueness of the pair potential is thus an almost trivial matter. The same does not hold, however, for its existence. Much more work needs to be done in order to find out, whether the search for a pair potential that reproduces a desired $g(r)$ is a quest worth beginning. Luckily, the answer is in the affirmative, as Chayes *et al.* have proven in their important papers from 1984.[72,73] The rigorous proof for the existence[72,73] is rather lengthy and will not be reproduced here. Basically, if the given RDF is a two-particle reduction of any admissible N-particle probability distribution, there always exists a pairpotential that reproduces it.[73] Admissible in this case refers to certain finiteness conditions. In addition, the above theorem holds even if the Hamiltonian of the system contains a fixed N-particle interaction term $W(x_1,\ldots,x_N)$ (satisfying certain conditions): any such W can be augmented by a pair potential such that the system reproduces the given RDF.

B Methods to solve the inverse problem

There are a number of different approaches to find a practical solution to the inverse problem (see, *e.g.*, ref. 76 and references therein). Most of these determine the pair potential with iterative adjustments, starting from an initial guess such as the potential of mean force $V_{\mathrm{PMF}} = -kT \ln g(r)$. Here, we focus on the inverse Monte Carlo (IMC) method introduced by Lyubartsev and Laaksonen in 1995.[77] We would also like to point out that there are new simplex-algorithm based optimization procedures developed by Müller-Plathe *et al.*[78–80] that exploit the above described relation. Next, we will focus on the IMC method, and in section IID we present two examples of how to use IMC to construct potentials for lipid membrane systems.

C The inverse Monte Carlo method—a simple case

We start by considering a single-component system with pairwise interactions only. In the following, we will also leave out the kinetic energy term, which has no bearing on this analysis. The Hamiltonian is then given as

$$H = \sum_{i,j} V(r_{ij}), \tag{2.4}$$

where $V(r_{ij})$ is the pair potential and r_{ij} is the distance between particles i and j. Let us assume that we know the radial distribution function (RDF) $g(r_{ij})$. Our aim is now to find the corresponding interaction potential $V(r_{ij})$.

To proceed, we introduce the following grid approximation to the Hamiltonian,

$$\tilde{V}(r) = V(r_\alpha) \equiv V_\alpha \tag{2.5}$$

for

$$r_\alpha - \frac{1}{2M} < r < r_\alpha + \frac{1}{2M} \text{ and } r_\alpha = (\alpha - 0.5)\, r_{\text{cut}}/M, \tag{2.6}$$

where $\alpha = 1,\ldots,M$, and M is the number of grid points within the interval $[0,r_{\text{cut}}]$, and r_{cut} is a chosen cut-off distance. Then, the Hamiltonian in eqn (2.4) can be rewritten as

$$H = \sum_\alpha V_\alpha S_\alpha, \tag{2.7}$$

where S_α is the number of pairs with interparticle distances inside the α-slice. Evidently, S_α is an estimator of the RDF: $\langle S_\alpha \rangle = 4\pi r^2 \rho(r) N^2/(2V)$. The average values of S_α are some functions of the potential V_α and can be written as an expansion

$$\Delta\langle S_\alpha \rangle = \sum_\gamma \frac{\partial \langle S_\alpha \rangle}{\partial V_\gamma} \Delta V_\gamma + \mathcal{O}(\Delta V^2). \tag{2.8}$$

The derivatives $\partial\langle S_\alpha \rangle/\partial V_\gamma$ can be obtained from a slightly generalized version of the fluctuation-response theorem of statistical mechanics:[77]

$$\frac{\partial \langle S_\alpha \rangle}{\partial V_\gamma} = \frac{\partial}{\partial V_\gamma} \frac{\int \mathrm{d}q S_\alpha(q) \exp(-\beta \sum_\lambda V_\lambda S_\lambda(q))}{\int \mathrm{d}q \exp(-\beta \sum_\lambda V_\lambda S_\lambda(q))}$$

$$= \frac{1}{k_{\text{B}} T} \text{Cov}(S_\alpha, S_\gamma). \tag{2.9}$$

Importantly, eqn (2.8) and (2.9) allow us to find the interaction potential V_α iteratively from the RDFs $\langle S_\alpha \rangle$. Let $V_\alpha^{(0)}$ be a trial potential for which the most natural choice is the potential of mean force

$$V_\alpha^{(0)} = -k_{\text{B}} T \ln \rho(r_\alpha), \tag{2.10}$$

where ρ is the density. By carrying out standard Monte Carlo simulations, one can evaluate the expectation values $\langle S_\alpha \rangle$ and their deviations from the reference values S^*_α defined from the RDF as $\Delta\langle S_\alpha \rangle^{(0)} = \langle S_\alpha \rangle^{(0)} - S^*_\alpha$. By solving the system of linear equations eqn (2.8) with coefficients defined by eqn (2.9), and omitting terms $\mathcal{O}(\Delta V^2)$, we obtain corrections to the potential $\Delta V_\alpha^{(0)}$. The procedure is then repeated with the new potential $V_\alpha^{(1)} = V_\alpha^{(0)} + \Delta V_\alpha^{(0)}$ until convergence is reached. This procedure resembles a solution of a multidimensional non-linear equation using the well-known Newton–Raphson method.

It may occur that the initial approximation of the potential is poor. In that case a regularization of the iteration procedure is needed. To accomplish that, we multiply the required change of the RDF by a small factor that is typically between 0 and 1. By doing so, the term $\mathcal{O}(\Delta V^2)$ in eqn (2.8) can be made small enough to guarantee convergence, although the number of iterations will increase.

Importantly, the above algorithm provides us also with a method to evaluate the error of the procedure. An analysis of the eigenvalues and eigenvectors of the matrix in eqn (2.9) allows one to make conclusions of which changes in $g(r)$ correspond to which changes in the potential. For example, eigenvectors with eigenvalues close to zero correspond to changes in the potential which have almost negligible effect on the RDF. The presence of these small eigenvalues makes the inverse problem not well-defined and in some cases may pose serious problems in the inversion procedure.[81]

There are a few important practical issues that must be considered. First, the Newton–Raphson approach rests on inverting the covariance matrix, which is only known approximately. If one is unlucky, inverting it amplifies these errors and the method does not converge. Second, convergence problems may arise if the number of degrees of freedom is large, and third, there may be "almost degenerate" potentials; the RDFs may look very different but give rise to rather similar pair potentials. It is possible, however, to limit these effects to a certain extent by using a regularization approach as discussed in ref. 82.

D Constructing the potentials: examples

As an example of constructing the potentials using IMC, let us consider a two-component model membrane consisting of phospholipids (DPPC, dipalmitoylphosphatidylcholine) and cholesterol. Length and time scales involved in large-scale structural reorganization of membranes are well beyond the reach of detailed simulations, similarly to the systems discussed in the Introduction. Thus, a coarse-grained simpler model is needed to assess the large-scale structure. Here, we will discuss two models that we have constructed.[82,83] It is also important to notice that the interaction potentials obtained using IMC can be used together, in a straightforward manner, with the dissipative particle dynamics thermostat which will be discussed in section IV. Interested readers will find an example of such a study in Lyubartsev *et al.*[84] We will now discuss IMC in membrane modeling.

Both models are based on similar ideas, namely, we focus on only one of the monolayers in the bilayer; that is justified when interaction between the two leaflets is weak. We then construct 2D models in which each molecule is described by one[83] or a few[82] particles. Each particle represents the center-of-mass position of (the part of) the corresponding molecule, and the target RDFs are calculated based on atomistic MD simulations of DPPC–cholesterol bilayers at several cholesterol concentrations using the IMC procedure as described in the previous sections. A separate set of potentials is constructed for each cholesterol concentration. The details of the atomistic simulations are reported in ref. 85. Briefly, the simulations were carried out at five different cholesterol molar concentrations (0%, 5%, 13%, 20%, 30%), with explicit water and with 128 lipid/cholesterol molecules at each simulation. Each simulation was run for 100 ns.

In the simpler model,[83] DPPC and cholesterol molecules are described by a single particle each, resulting in two particle types and three distinct interaction potentials. In the second model,[82] each cholesterol is still described by a single particle,

but three particles are now used for DPPC. One of the particles describes the headgroup, and the two others the tails, *i.e.*, the acyl chains. In addition to the non-bonded interactions, the model includes three distinct bonded interactions, one between each pair of particles in a DPPC. For intramolecular tail–tail and tail–cholesterol interactions, all the tail particles are treated as identical. In total, this results in a model with four particle types, seven non-bonded interactions, and three bonded interactions. The model is still completely two-dimensional; the fact that the headgroup and the tails occupy mostly separate regions in space is reflected only in the weakness of the interaction between such non-bonded pairs. For a detailed discussion of the models, the reader is referred to the original publications.[82,83]

One additional point about the three-particle model is worth noticing: at high cholesterol concentrations, the interactions derived using the standard IMC result in unphysical behavior for large systems.[82] This is also visible in the 2D pressure of the CG model, which is significantly negative for the highest cholesterol concentrations. To obtain physical interactions, we have implemented an additional constraint to the IMC procedure which forces the 2D pressure to take a determined value. Details can be found in ref. 82. Varying the target pressure results mostly in changes in the interactions involving the particles representing the head groups of lipids, while other interactions (as well as qualitative results) are largely independent of the target pressure, as long as the pressure is positive.

Fig. 3 shows the effective potentials constructed for cholesterol–cholesterol pairs for both models. At each concentration, the general shape of the potentials is similar for the model. The same holds when comparing the changes between concentrations between different models. However, the potentials are more attractive for the model with three particles per DPPC. Also, there is more structure in the potentials for the simpler model, *i.e.*, there are more local minima at larger separations than with the three-particle model. Hence, although the definition of a cholesterol particle is identical in both models (*i.e.*, the target cholesterol–cholesterol RDF is the same), changes in other properties of the model also change the cholesterol–cholesterol RDFs. The reduction in the number of local minima in the potentials indicates that the three-particle model is better able to capture the underlying structural features of the system, because the cholesterol–cholesterol interaction no longer needs to create the structure at length scales much longer than the nearest-neighbor distance.

Both of the models allow simulations of the structure of membrane patches whose linear size is of the order of 100 nm. Fig. 3 shows snapshots of how the cholesterol molecules organize at different cholesterol concentrations. A snapshot from two cholesterol concentrations, 13% and 30%, is shown for both models. The snapshots indicate, and other quantities confirm,[82,83] that at 30%, the cholesterol distribution is uniform, but at 13%, there are regions of higher and lower density. Also, the difference is substantially larger with the more detailed model. At 20% concentration, the distribution is similar to 13%, *i.e.*, not uniform, while at 5%, the distribution is uniform.[82,83] This in agreement with the phase diagram of the binary mixture, based on which coexistence of cholesterol-poor and cholesterol-rich phase is expected at intermediate cholesterol concentrations.

In addition to the cholesterol results above, the model with three particles per DPPC predicts interesting behavior for the pure DPPC system:[82] the chains seem to form denser and sparser domains (results not shown). After the CG model studies, we have confirmed that this also occurs in large-scale atomistic simulations of the same system.[86]

Both the organization of cholesterol and the results for the pure DPPC show that even such a simple model, if carefully constructed, can be used to extract at least qualitative information on the behavior of the system at much larger length scales than those accessible through atomistic simulations. Quantitative analysis with such a simple model is not straightforward, however, as the exact quantitative behavior can depend on details of the interactions.[82]

Also, the comparison between the different models gives some insight into the effect of the degrees of freedom selected for the model. The formation of cholesterol-rich and cholesterol-poor domains is much stronger in the model in

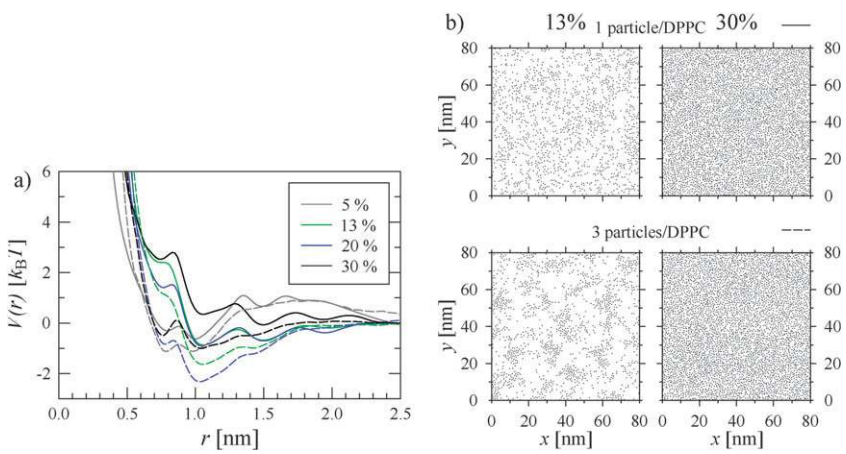

Fig. 3 (a) Cholesterol–cholesterol effective potentials for different cholesterol concentrations. Solid line corresponds to the simpler model (one particle/DPPC), and the dashed line to the three-particle model. (b) Distribution of cholesterol for both models at 13% and 30% cholesterol concentrations. Each dot represents a single cholesterol molecule, and the rest of the particles are not shown.

which the tails are represented explicitly, and also the strong density fluctuations in pure DPPC are only captured by the more detailed model. The issue of selecting the degrees of freedom is discussed in some more detail in section III.

E Is there more to pair potentials?

RDF-based inversion discussed above is not the only possible approach for constructing the effective potentials systematically from a detailed model. It is also possible to calculate the forces on coarse-grained particles from a detailed model, and minimize the difference between the detailed force and the coarse-grained force. This is the basis of the force matching procedure recently developed by Voth and co-workers.[87–89] In the context of biological systems, the method has been applied to construct semi-atomistic models for phospholipid bilayers with and without cholesterol,[90,91] for monosaccharide solutions,[92] for short peptides in water[93] and even an atomistic protein within a coarse-grained bilayer.[94]

To compare the methods more closely, it is useful to define exactly what we would like to achieve with systematic coarse graining. The logical definition is the reproduction of the equilibrium probability distribution functions of the coarse-grained coordinates[95] (for this discussion, we neglect the momentum part of the Hamiltonian). Following the presentation by Noid *et al.*,[95] let $\mathbf{R}^N$ be the coarse-grained degrees of freedom and $\mathbf{r}^n$ the detailed degrees of freedom, and define a mapping operator $\mathbf{M}^N$ that maps the detailed model to the coarse-grained model: $\mathbf{R}^N = \mathbf{M}^N(\mathbf{r}^n)$. We can then define the coarse-grained model to be exactly consistent with the detailed model if[95]

$$\exp\{-\mathrm{U}(\mathbf{R}^N)/k_\mathrm{B}T\} \propto \int \mathrm{d}\mathbf{r}^n \exp\{-u(\mathbf{r}^n)/k_\mathrm{B}T\}\delta(\mathbf{M}^N(\mathbf{r}^n) - \mathbf{R}^n), \qquad (2.11)$$

where U and u are the potential energy functions of the coarse-grained and the detailed model, respectively (U is actually a free energy, as is evident from the form of eqn (2.11)). If this condition holds, any quantity that depends only on the coarse-grained positions $\mathbf{R}^N$ can be calculated exactly from the coarse-grained model, *i.e.*, the result is the same as from the detailed model. Noid *et al.* have carefully analyzed the conditions that the mapping $\mathbf{M}^N$ has to satisfy to allow eqn (2.11) to hold,[95] and here it is sufficient to note that for a typical mapping that uses the centers of mass of groups of atoms, these conditions are always satisfied.

The relationship of force matching to eqn (2.11) is simple, and is analyzed in detail in ref. 95 & 96: if we take the logarithm (*i.e.*, calculate the free energy) and differentiate with respect to $\mathbf{R}^N$, the left side becomes the total coarse-grained force, and the right side becomes the average atomistic force (evaluated keeping the $\mathbf{R}^N$ fixed). For the RDF-based method, it follows from the form of the Hamiltonian in eqn (2.7) that the RDF, *i.e.*, the target function, is the derivative of the free energy with respect to the coarse-grained potential. Hence, both methods use derivatives of the free energy as their target function in constructing the coarse-grained interactions. For force-matching, the target function is the derivative of the constrained free energy $U(\mathbf{R}^N)$ with respect to the positions $\mathbf{R}^N$, while RDF-based methods use the derivative of the total free energy with respect to the coarse-grained potential.

Another view on the similarities and differences between the two approaches has been provided by Noid *et al.*[96] They showed that for a homogeneous, isotropic system with a central pair potential, the force matching equations are in fact identical to the Yvon–Born–Green (YBG) equation.[40] For a fluid with a central pair potential, the YBG equation provides a relationship that links the force to the two- and three-particle correlation functions. Hence, the force matching algorithm provides an effective potential that, assuming that such a potential would exist, reproduces both the two- and three-particle correlation functions. Typically, such a potential does not exist, and the force-matched interaction does not produce either correlation function exactly. Instead, it is a solution to *two* YBG equations, one with the atomistic correlation functions and one with the actual coarse-grained ones. In contrast, the RDF-based effective interaction reproduces the two-particle correlation function exactly, but does not guarantee anything about the three-particle correlation function.

The above discussion naturally leads to the conclusion that there typically is no single effective (pairwise) interaction that could reproduce all the quantities of interest. Instead, one has to choose the method for constructing the interactions based on what one wants to study,[97] also taking into account the possibly different computational costs of the different alternatives.

Another issue to note about the effective interactions is that the interactions are specific to the state point in which they were constructed. This is an inherent property of the coarse-graining process, and is not related to the pairwise assumption; indeed, it is clearly seen from eqn (2.11) that the optimal effective interaction U is a free energy, and as such, depends on the thermodynamic state. However, interactions constructed in different ways can have different transferability properties, and careful study is needed on a case-by-case basis.

As a final point, we would like to briefly discuss other approaches to coarse graining where the requirement for exact match with the atomistic model is relaxed, and macroscopic quantities are used as the target. This is the leading idea behind the MARTINI force field,[18–20] where thermodynamic quantities have been used in the parameterization. Because the input information in these approaches is less detailed, the functional form of the pairwise forces is assumed to be, *e.g.*, of the Lennard-Jones form, and the interaction parameters are fitted to reproduce experimental densities and other quantities of interest using simulations of model substances. This process resembles the parameterization of atomistic force fields. In the MARTINI model, the partition free energies between water and oil have been taken as the target quantities. This also aims to reproduce the free energy of the detailed system, although in a much more heuristic fashion. Hence, the (quantitative) agreement with atomistic models is not as good as with models constructed from RDFs or the forces, but on the other hand, the dependence on the thermodynamical state may not be as strong as with the more detailed CG models, because it does not explicitly enter the parameterization (there are still issues, because typically at least some of the target quantities depend

on temperature). Indeed, the MARTINI force field has been successfully used to study phase behavior of lipid systems: it qualitatively reproduces the main phase transition of lipid bilayers,[98] as well as the lamellar to inverted hexagonal transition.[99,100] It has also been successfully applied to studies of monolayers as a function surface tension.[101]

III. Coarse graining of molecular structures with self-organizing maps

A Introduction to SOMs and clustering in coarse graining

The degrees of freedom used for a coarse-grained model can have a profound effect on the properties of the model. In principle, a good choice of interactions can remedy some deficiencies in the degrees of freedom, but in practice, computational considerations limit the interactions to relatively simple forms. As a simple example, interactions between particles are typically chosen to be pairwise and isotropic. In such cases, if the particles are not chosen to describe approximately spherical parts of the system, the model may not be able to adequately describe the underlying system. Hence, methods for evaluating the quality of the selected degrees of freedom, and in particular methods for finding good degrees of freedom, are of great interest for coarse graining. One major goal would be to select the degrees of freedom based on information from a more detailed model. For example, atomistic simulations provide a wealth of data on the structures and interactions in the system, and systematic methods for using this data for selecting the coarse-grained description would provide an attractive alternative for the more *ad-hoc* methods, in many cases just educated guesses, that are currently used.

Several methods developed in the context of data analysis may yield information useful for coarse graining. The relationship is perhaps the most direct for dimensionality-reduction techniques, where one tries to construct a mapping of the data points onto a lower dimensional space while trying to preserve, *e.g.*, distances between the data points. Such techniques could be applied to, *e.g.*, internal coordinates of a macromolecule to distinguish characteristic conformational changes from local fluctuations.[102–104] Traditional methods such as principal component analysis are linear, and are not always suitable for analysis of complex data where the relationships are typically non-linear.[105] Traditional non-linear projection techniques, such as Sammon mapping, can be computationally costly for large amounts of data. However, in many cases only local similarity is important and longer distances do not need to be preserved in the mapping. Recent methods such as locally linear embeddings and diffusion maps take advantage of this to find the local geometry of a submanifold on which the data approximately lies.[106–109]

Clustering methods provide a somewhat different approach.[110,111] These methods try to classify the data into clusters such that points within one cluster are similar to each other and dissimilar with points in the other clusters. The clusters can then be represented using simpler representations, *e.g.*, average conformation within the cluster, and analysis of the clustering can yield information on the typical features of the data.[110,111] Such information could also be used to design coarse-grained models that are able to represent the major differences between the clusters, in the hope of being thus able to capture the rough features of the original system.

Let us now focus on self-organizing maps (SOMs),[112] which is an approach somewhere in between dimensionality reduction and clustering. In essence, it is a mapping from the input data onto a (typically) two-dimensional output space such that similar data points are generally mapped to locations close to each other. The SOM itself consists of a grid of model vectors, also called neurons, each describing a set of data vectors. In other words, each neuron has two conceptually different "positions" associated to it: the neurons lay on a 2D grid in the output space, and the model vector describes some kind of average conformation associated with the neuron. The former define the topology of the map, and do not change at any point, while the latter are first initialized to some values and then modified in a process called training. The training algorithm is inspired by studies of learning in the brain. Hence, SOM can be thought of as a neural network-based approach.[113] The training method is unsupervised, *i.e.*, no *a priori* knowledge of the data is needed for constructing the map. After the training, each data vector can then be associated with the neuron whose model vector is most similar, resulting in a grouping of the data that can easily be visualized using the 2D positions of the neurons.

The map is constructed by first initializing the model vectors either randomly or based on the variance of the data.[112] The map is then trained by sequentially selecting a data vector, finding the neuron whose model vector that is most similar to it (the so-called best-matching unit, BMU), and updating that model vector as well as those of the neighboring neurons to be more similar to the data vector. The equation used in the update process has the form

$$\boldsymbol{m}_i = \boldsymbol{m}_i^0 + \alpha(t)h_{i,\mathrm{BMU}(\boldsymbol{x})}(t)(\boldsymbol{x} - \boldsymbol{m}_i^0), \qquad (3.1)$$

where $\boldsymbol{x}$ is the data vector, $\boldsymbol{m}_i^0$ and $\boldsymbol{m}_i$ are the model vectors before and after the update, $\alpha(t) \in [0,1]$ sets the magnitude for the change, and $h_{i,j}(t)$ is a so-called neighborhood function that determines how the model vectors near the BMU are updated. $h_{i,j}$ is a decreasing function of the distance between the neurons, such that the changes are the largest for the BMU, and decrease as model vectors farther away in the map are considered. Note that the 2D distance between neurons is used in the neighborhood function, forcing the model vectors of neurons that are close to each other in the output space to change in a generally similar fashion. t represents the time that has passed since the beginning of the training, and the functions α and h are such that in the beginning of the training, each data vector results in large changes of the BMU as well as a relatively large neighborhood, while towards the end of the training, only small changes to the BMU, and perhaps its nearest neighbors, are made. Fig. 4 illustrates the training step for a single data vector $\boldsymbol{x}$.

An intuitive picture of a two-dimensional SOM is a stretchable membrane that is stretched such that it tries to adopt the distribution of the data points. Initially, the

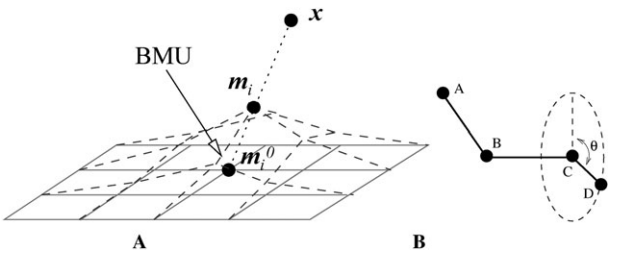

Fig. 4 (A) Schematic diagram of SOM training step with data vector $\boldsymbol{x}$. BMU (best-matching unit) is the model vector that is most similar to $\boldsymbol{x}$ and $\boldsymbol{m}_i^0$ and $\boldsymbol{m}_i$ are the model vectors before and after the update. Each model vector is made more similar to the data vector, the magnitude of the change determined by the learning rate α and the proximity of the BMU (in the topological sense, *i.e.*, using the positions of the neurons on the 2D grid) through the neighborhood function $h_{i,j}$ (see text for details). (B) Illustration of a dihedral angle.

membrane is planar and the tension is high. During training, each data point pulls the nearest point on the membrane. As the training proceeds, the tension is relaxed and the membrane is able to adapt to finer features of the data. For technical details, as well as discussion of the different training parameters, the reader is referred to ref. 112 and 114. Ref. 114 also explores the effect of the training parameters on the results, and gives reasonable values that are applicable (at least) to lipid systems.

As discussed above, SOM is only one method that could be used to extract information useful for coarse graining. We have chosen to study it in more detail for several reasons. First, the unsupervised nature of the method makes it ideal for analysis of complex data where it is difficult to establish *a priori* what might be the most important features. Second, the SOM results are easy to visualize since the output space is two-dimensional. The visualization methods developed for SOMs are a powerful tool in finding non-trivial characteristics of the data, also for assessing the validity of the results. Finally, SOMs are relatively easy to implement, and a comprehensive SOM Toolbox is freely available for the MatLab environment.[115] The computational cost of SOMs is also modest, although training a big map with a large amount of data can take a few days. In many ways, SOM is more qualitative than many other approaches, but this is not just a disadvantage; this allows a careful interpreter to get around other limitations of the results up to a certain extent, in particular since the training algorithm and its possible effects on the final map are relatively easy to understand.

B Example application to a membrane system

Let us now focus on a particular application of SOMs to a PLPC bilayer. Full account of the analysis is presented in ref. 114, and here we show some additional results and discuss the application to coarse graining in detail. The conformations for the analysis were obtained from a 50 ns simulation of 128 fully hydrated lipid molecules (total of $\sim$500 000 conformations), and the conformations were described using dihedral angles, *i.e.*, angles that describe rotations around bonds (see Fig. 4). The molecule was analyzed in parts to reduce the computational cost, in particular the size of the map that is needed to describe the conformational space adequately.[114] A map with 48 $\times$ 72 neurons was trained for each region, and the results were visualized and analyzed. A visualization of the map typically consists of the 2D grid of neurons colored and/or labeled based on some quantity.

Fig. 5 shows the map trained for the headgroup region consisting of 12 dihedral angles,[114] together with some quantities visualized on the map; only the dihedral angles of the molecule have been used to train the map. In the first sub-Figure, Fig. 5 shows the unified distance matrix (U-matrix), in which different regions are colored based on local similarity: light colors denote regions where the neighboring model vectors are similar to each other, and in darker regions the differences are larger. The second and the third sub-Figure visualize average orientations (with respect to the bilayer normal) of the conformations mapped to each neuron. The second sub-Figure shows the average angle between the P–N vector (from the phosphorous atom in the head group to the nitrogen atom in the same entity) and the bilayer normal, while the third sub-Figure shows the average angle between the glycerol plane (formed by the three carbons) and the bilayer normal. For both Figures, the sizes of the symbols are proportional to the number of conformations for which that model vector is the most similar. Note that orientational data has not been used in training of the map.

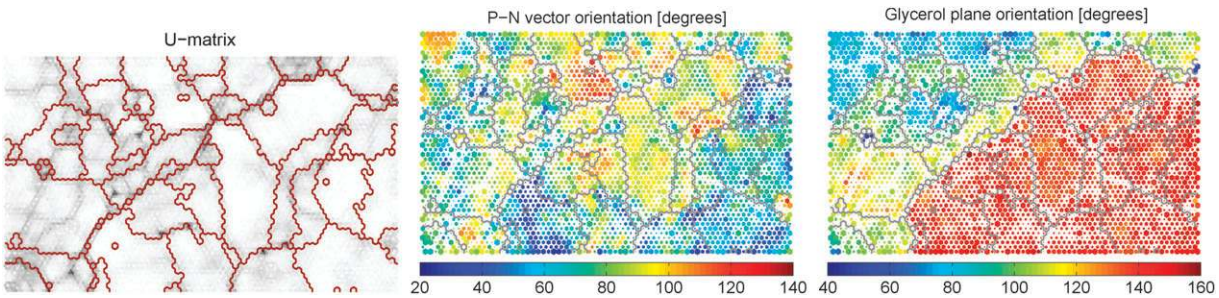

Fig. 5 Visualization of selected SOM results for headgroup region of PLPC. The first sub-Figure shows the U-matrix; light colors denote regions where model vectors are similar to their neighbors, while darker regions mark larger differences. The color in the second sub-Figure shows the angle between the P–N vector and the bilayer normal, while the right-handfigure shows the angle between the bilayer normal and the normal of the glycerol plane (defined by the three glycerol carbon atoms). The sizes of the symbols are proportional to the number of configurations represented by the neuron. Each map is divided into distinct regions based on the dynamics of the lipids as described in ref. 114. Note that only the dihedral angles of the molecule have been used to train the map, *i.e.*, the quantities shown have not been used.

The U-matrix in Fig. 5 shows several light-colored clusters separated by darker boundaries. Some of the boundaries are stronger, such as the one dividing the map from the lower left corner to the upper right corner. This boundary is also clearly seen in the orientation of the glycerol plane, and it divides the map into two parts with different structure: the bottom half has a small number of large clusters, while the upper half varies more. Many of the cluster boundaries also correspond to clear changes in P–N vector orientation, the glycerol orientation, and/or the angle between the P–N vector and the vector connecting the first carbons in the acyl chains (the last one not shown). Although only intramolecular information has been used in training the data, the map also captures several orientational characteristics of the molecules.

In general, analysis such as the one presented in Fig. 5 gives insight into the typical conformations of the headgroup region in the studied lipid bilayer.

Similar analysis can also be done for other parts of the molecule, and the results can be combined to get an overview of the most relevant conformational degrees of freedom of the whole molecule.[114]

How could such information then be used in coarse graining? As outlined above, the knowledge of the features that distinguish the major conformations from each other can be used to select a minimal model that contains these features. For the case of PLPC, the basic idea of such a deduction is shown in Fig. 6 for the case of a semi-atomistic model. To arrive at the description shown in Fig. 6, we focus separately on the headgroup/glycerol region and the tail, as SOM shows very different behavior in these regions.[114]

The maps for the headgroup and the glycerol regions show very similar structure, partly due to the fact that they share some of the dihedrals used in the training.[114] Looking at the model conformations of the clusters, as well as the data shown in Fig. 5, it seems that the most important conformational feature of the headgroup is the orientation of the P–N vector with respect to the glycerol backbone. For the glycerol region, the orientation of the chains with respect to the glycerol backbone is a similar factor. For both maps, one of the most important factors in dividing the map into clusters is the orientation of the glycerol plane. A minimal representation that could describe these conformations should contain three to four atoms: two to define the orientation of the P–N vector, and one to two for describing the glycerol region. The glycerol region itself does not seem to have any significant internal degrees of freedom, but seems to act as a joint between the headgroup and the chains. However, the joint is not necessarily freely rotating, as indicated by a clear division of the conformations into clusters. Hence, if the conformations need to be reproduced accurately, care should be taken in determining the intramolecular interactions, in particular if only one particle is used for the glycerol region.

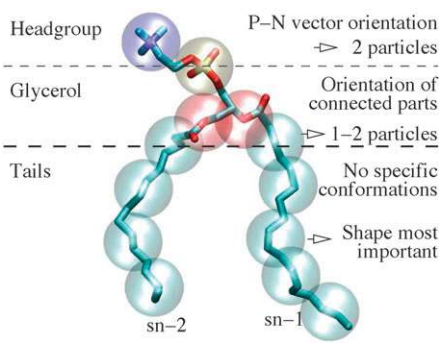

Fig. 6 Schematic description of how SOM data could be used in constructing coarse-grained representations (see text for details). Adapted from ref. 114.

For the chains (*sn*–2 analyzed in ref. 114), the trained SOM is very homogeneous. This indicates that there are no specific favored conformations, not even in the chain with the double bonds. Hence, the general shape of the chains should be the only concern for selecting the representation, and the differences between saturated and unsaturated chains only come into play at the intramolecular interactions.

For a complete model, the interactions between the different particles should also be determined. Any systematic method, such as the structure-based schemes discussed earlier, could be used for this, but such analysis is beyond the scope of the present discussion. It is also interesting to note that many successful coarse-grained models for lipid systems, such as the one developed in ref. 18, incorporate the main features seen in SOM analysis of atomistic structures. The earlier models used knowledge and experiences from extensive atomistic simulations, and the fact that SOM analysis can provide similar information demonstrates its potential as an aid in designing coarse-grained models. SOM analysis also indicates that special attention needs to be paid to the glycerol region if the conformations need to be accurately reproduced.

C Further discussion

The application of SOM to coarse graining is still on a very preliminary level, as also exemplified by the general nature of the discussion above. Nevertheless, the potential of SOM has been scarcely explored even in the (somewhat simpler) context of conformational analysis: there exists an SOM study which analyzes the 3D structure of amino acid sequences,[116] as well as another preliminary application of SOM to lipids.[117] Instead of directly analyzing the conformations, SOM has been applied to higher-level data. For example, most SOM studies of proteins have focused on analysis on the sequence level. Examples include sequence classification within a protein family,[118] identification of overrepresented motifs in sequences,[119,120] prediction of HIV protease cleavage sites,[121] and a study of ammonium salts as ligands of the neuronal nicotinic acetylcholine receptor.[122]

The results from basic SOM analysis, such as those shown in Fig. 5, can also be used as a basis for further analysis. For example, more quantitative analysis of the clusters can be done, or other clustering algorithms could be applied to the SOM model vectors.[114,123] The dynamics of the molecules can also be studied by analyzing the trajectories of the molecules on the map.[114] The map itself could also possibly be used for assessing correlations between nearby molecules, or a separate map could be trained to study such phenomena by including intermolecular variables into the data. This could give insight, *e.g.*, into specific interactions between the molecules. All these

additional studies can yield more information for interpretation of the results, and also give knowledge for designing better coarse-grained models.

A significant amount of the discussion in this section is not specific to SOM; other methods, such as more traditional clustering methods, could be applied to a similar end. The pros and cons of SOMs were discussed in the introduction, and only future work will show which of the methods proves best for a particular purpose.

So far, we have dealt with two important issues regarding coarse graining in general, namely how the coarse-grained description of a molecule can be derived in a systematic manner, and, once the coarse-grained description is available, how the effective potentials can be derived for the coarse-grained model. Next, we will describe one of the topical and particularly appealing methods that have been developed to model complex systems in a coarse-grained manner: dissipative particle dynamics (DPD). Due to a number of features characteristic to DPD in particular, we focus here on methodological issues with a purpose to clarify the conditions under which DPD can be employed. These considerations are complemented by discussion of some applications where DPD has recently been used with success.

IV. Dissipative particle dynamics (DPD)

Dissipative particle dynamics (DPD) is the most commonly used and possibly the easiest to implement of the mesoscopic simulation methods. The definition of DPD, however, is not consistent throughout the literature and we will therefore begin with a clarification: "classical" DPD consists, as it was originally envisioned, of two separate ideas which are fused for purely historical reasons: (1) a pairwise thermostat which preserves local momentum and Galilean invariance; and (2) a set of rather simplistic soft potentials. The overwhelming and, ultimately, lasting success of DPD is largely due to the first concept, while the second is not actually particularly profound on its own, even though it has resulted in a variety of very useful and important publications to be discussed below. We would like to, in this review, encourage a different terminology: DPD refers to "the DPD thermostat" isolated from any specific set of potentials.

When simulating at constant temperature, some of the most commonly used thermostats, such as the Nosé–Hoover,[124–126] Berendsen,[127] or Andersen thermostats[128] only conserve the average momentum of the entire system, but not the local momentum, and they are applied globally, *i.e.*, everywhere instantaneously and with the same strength. If this is good enough in a detailed MD simulation, why do we need the extra criterion of local momentum conservation and Galilean invariance? The answer lies in the time and length scales that can be simulated using soft potentials. MD is commonly used for all atom simulations where one is limited to time scales of up to 100–200 ns at best and system sizes with the linear dimension of about 6–15 nm. Coarse grained potentials, however, are commonly used to model length and time scales of micrometers and microseconds. Then, hydrodynamic effects, that can be neglected at the scales accessible using conventional MD, become important as shown by Groot and Warren.[129] It has also been shown[130,131] that local momentum invariance of the thermostat is important for non-equilibrium molecular dynamics simulations. Whenever the relaxation of a soft system requires large cooperative distributions of particles, a pairwise noise-and-friction term will hardly impede a cooperative motion of a large patch (because all relative velocities are close to zero).

Let us quickly point out the main advantages and disadvantages of DPD. The DPD thermostat with coarse-grained potentials differs in several ways from the competing mesoscale modelling methods, which include the dynamic mean field density functional method,[132] stochastic rotation dynamics,[48] lattice-Boltzmann (LB),[133,134] and the Voronoi fluid particle model.[135] Unlike LB it does not discretize the system to a grid, thus inducing a possible artificial anisotropy to the system, and unlike other methods mentioned, which involve free particles, it is flexible, easy to implement, and can be modified to be applied to a wide range of physical systems. The main disadvantages arise from: (1) for the case of constant-temperature simulation, solving equations of motion using a thermostat that explicitly conserves local momentum; (2) the washing-out of important microscopic structural detail that may affect the results on the mesoscopic scale; and (3) the phenomenological nature of the interaction parameters. The latter two apply to most of coarse graining, not just DPD. There has been considerable recent progress on resolving these three issues and we will later focus on recent efforts to resolve them.

The concept of DPD was first devised in 1992 by Hoogerbrugge and Koelman,[136] however the form of the equations of motion they developed was incomplete. In addition, their numerical solution to the equations of motion made use of an Euler algorithm which violates time reversibility. This was corrected by Español and Warren[137,138] and Warren, who in collaboration with Groot, went on to present the first workable numerical algorithm[129] to solve the DPD equations of motion.

The soft potentials originally used alongside the DPD thermostat model the intermolecular conservative forces through two body soft core interactions with a cutoff r_c of the form:

$$\mathbf{f}_{ij}^{C} = \begin{cases} \alpha_{ij}(1 - r/r_c)\,\hat{\mathbf{r}}_{ij} & r \le r_c \\ 0 & r > r_c. \end{cases} \qquad (4.1)$$

Typically, one chooses $r_c = 1$. In the original incarnation of the DPD thermostat, constant temperature was provided by random and dissipative forces acting between particles closer than the interaction cutoff, effectively a momentum conserving Langevin thermostat. All particles had mass ($m = 1$) and represented carriers of equal-sized packets of momentum. In the simulation there would be several different particle types and the interaction parameter α_{ij} would govern the affinity of each pair combination. Groot *et al.*[139] devised a formalism, where, given that the mass and length scale have been set (unit mass and particle cutoff $r_c = 1$), all α_{ij} values could be extracted from a combination of fitting to this scaling and the experimental results for the mutual solubility χ parameters. This method for the determination of the α_{ij} values has since

been found to create inaccurate results for several cases[140] and other, more accurate formalisms have since been proposed.[141]

With only the above interactions DPD is restricted to observing the trivial problem of phase coexistence and separation of binary fluids with mutual solubility parameter χ. The first step made towards developing this into an algorithm that can be used to simulate a real system was insertion of harmonic "springs" between particles by Schlijper *et al.*[142] to simulate mesoscopic "bead-spring" models of polymers. The behavior of such a model of a polymer melt was examined by Spenley,[143] who showed the dynamics to obey Rouse dynamics, over the full range of polymer lengths without the expected crossover into reptation dynamics of the bead spring model. The reason for this is that the soft DPD interactions are too soft to inhibit chains from crossing through each other. Recently techniques have been developed to rectify this failing of the model by adding specific interactions to inhibit chain crossover,[144,145] though for a large class of complex fluids this is not necessary because:[146] (1) the chain lengths of the polymers involved are short enough or the system is dilute enough for their dynamic behavior to be Rouse-like; and (2) the rheology of these systems is dominated by the self organization of microstructure resulting from phase separation instead of polymer chain dynamics. One of the most relevant mesoscopic phenomena of a complex fluid is its rheology, and studying rheology through the application of shear to a DPD system was one of the main initial purposes of the development of the method. Some of the earliest DPD studies have been of the shear rheologies of fluids.[147,148] The application of shear to a DPD simulation through the use of Lees–Edwards boundary conditions has been concisely described by Sims and Martys.[149]

The original conception of DPD described above has been successfully applied to model a wide variety of soft matter systems, including block copolymers,[150,151] oil/water/surfactant systems,[152] polymer surfactant solutions,[153] multi-component fluids,[154] bilayer membranes[155] (including cell membranes[139]) and vesicles.[156,157] A particularly fruitful field of study has been the study of mesoscopic structures made up of lipid membranes. In one of the first applications of the parameterization of DPD with the solubility χ parameters Groot and Rabone[139] showed that the presence of surfactant molecules greatly diminishes the stress and extensibility of a phospholipid bilayer, and Yamamoto *et al.* demonstrated the spontaneous formation of lipid vesicles.[158]

It is at this point that we feel it is very important to dispel several further common misconceptions concerning DPD simulation. We are not limited to NVT; a technique to perform DPD simulation with either constant pressure or constant surface tension has been developed and applied by Jakobsen *et al.*[159] This is in fact not such a difficult problem, as any barostat which varies the box size isotropically will maintain the transport phenomena of the DPD system. A more elegant barostat than that proposed by Jakobsen *et al.*, that also could be applied to DPD simulation, but as of yet has not been is the isotropic barostat of Kolb and Dünweg.[160] We are also not limited to soft single parameter intermolecular forces or uniform particle mass and force cutoff as the DPD thermostat has been used outside of this context.[161] Intra-molecular forces other than harmonic "springs" have been implemented including 2–4 interactions,[140] FENE springs[161] and the accuracy of the surfactant simulation has been increased by Shillcock *et al.*[155] through the addition of a three body potential acting between consecutive bead triples. We are finally not limited to the thermostating being provided by dissipative and random forces, as the now widely used Lowe–Andersen themostat[162] and the extension of this method proposed by Stoyanov and Groot[163] attest.

One final warning seems appropriate: The use of the DPD thermostat with, in particular, soft interactions has encouraged people to use substantially longer integration time steps than are typically employed in conventional simulations with harder potentials, such as Lennard-Jones. Indeed, Groot and Warren showed that a time step roughly five times longer than the conventional $\tau = 0.05$ (in reduced units) suffices to achieve 1% accuracy in kinetic temperature.[129] When using additional interactions, however, such as bonds between DPD particles, this state of affairs ought to be carefully revisited. Indeed, Allen has shown that in some cases the resulting inaccuracies are disastrous:[164] even if the kinetic temperature is within a few percent of its target value, the configurational temperature (derived *via* a hypervirial condition) can be off by more than a factor of 2.

Before going to the technical matters, let us finish this discussion with an example. Shillcock and Lipowski used the "classical DPD" (soft potentials and thermostat) to study tension induced fusion of vesicle membranes.[156] Artificial vesicles are very promising for drug delivery and in order for the vesicle to deliver the desired contents to a cell, the membranes of the cell and the vesicle must fuse. Since cell membranes must maintain their integrity for the cell to survive, and vesicles used for drug delivery must stay intact until the cell is reached, there clearly exists an intrinsic resistance to membrane rupture and fusion. Shillcock and Lipowski used a coarse-grained representation with the DPD thermostat of a 30 nm diameter vesicle interacting with a 50 nm wide section of membrane. They monitored the time evolution of 93 fusion attempts and characterize the dependence of fusion on the initial tension within the vesicle and membrane. They were able to determine that fusion induced by relatively large tension occurs on the timescale of roughly 350 ns. This kind of studies of large system sizes and long time scales are only possible using coarse-grained methods; as a comparison, using classical MD, it has been possible to study micellation[165–168] and micelle fission[169] in systems only up to a few hundred surfactants (the difference is, though, that one obtains very detailed information from MD simulations). In addition to DPD, other coarse-grained models have been applied to micelles and vesicles, see *e.g.* ref. 170.

The current activity in the field of using the DPD thermostat to study biological and soft matter systems is far too great to be comprehensively covered here. A demonstration of its breadth is made by these 10 articles published between May and September of 2008 alone.[171–180]

A Deriving and solving the DPD equations of motion

Thermostating in DPD using random and dissipative forces can be seen as making use of a momentum conserving

Langevin thermostat. In the Langevin thermostat all particles are subjected to dissipative forces (F_I^C) and random impulses ($\dot{\mathbf{p}}_i^R$). As a result the particle dynamics will be governed by the Langevin equations of motion:

$$\dot{\mathbf{r}}_i = (\mathbf{p}_i/m_i) \tag{4.2}$$

$$\dot{\mathbf{p}}_i = \mathbf{F}_i^C + \mathbf{F}_i^D + \dot{\mathbf{p}}_i^R, \tag{4.3}$$

where the conservative, frictional, and random forces are given by

$$\mathbf{F}_i^C = \sum_{i \neq j} \mathbf{f}_{ij}^C \tag{4.4}$$

$$\mathbf{F}_i^D = -\Gamma \dot{\mathbf{r}}_i \tag{4.5}$$

$$\dot{\mathbf{p}}_i^R = \xi_i(t). \tag{4.6}$$

Here, $\xi_i(t)$ is a Gaussian white noise correlated noise with zero mean and a variance adjusted *via* the fluctuation–dissipation theorem to reproduce the fluctuations present in the canonical state:

$$\langle \xi_i(t) \rangle = 0 \tag{4.7}$$

$$\langle \xi_i(t) \xi_i(t') \rangle = 2k_B T \Gamma \delta_{ij} \delta(t - t'). \tag{4.8}$$

The Langevin thermostat can thus be seen to mimic the presence of a viscous medium, with Γ being the coefficient of the induced drag and the random impulse representing random collisions with Brownian particles within the medium.

The random impulses and dissipative forces of the Langevin thermostat are incorporated, but instead of applying them to the individual particles independently, hence losing the local momentum conservation, the dissipative forces and random impulses are applied through pairwise interactions between the particles. The DPD equations of motion have the same form as the Langevin equations of motion, however the dissipative forces and random impulses are now given by

$$\mathbf{F}_i^D = -\gamma \sum_{i \neq j} \omega_D(r_{ij}) (\dot{\mathbf{r}}_{ij} \cdot \hat{\mathbf{r}}_{ij}) \hat{\mathbf{r}}_{ij} \tag{4.9}$$

$$\dot{\mathbf{p}}_i^R = \sigma \sum_{i \neq j} \omega_R(r_{ij}) \hat{\mathbf{r}}_{ij} \dot{W}, \tag{4.10}$$

where γ and σ are the coefficients of dissipative and random force, respectively, $\omega_R(r_{ij})$ and $\omega_D(r_{ij})$ are functions specifying the strength of noise and dissipation in a distance dependent fashion, and $\dot{W}$ is the time derivative of a Wiener process. As far as we are aware, there are only two publications in which the weight function is approached in a systematic fashion.[181,182]

It has been shown by Español and Warren[137] that in order to satisfy the fluctuation dissipation theorem, and thus recover the Gibbs distribution as a stationary solution to the Fokker–Planck equation, the following relations must hold

$$\omega_D(r_{ij}) = (\omega_R(r_{ij}))^2 \tag{4.11}$$

$$\sigma = \sqrt{2\gamma k_B T} \tag{4.12}$$

thus reducing four free parameters to two. They also found that this only applies in the limit of small time step of the numerical algorithm applied to solve the DPD equations of motion. So far in its application the most common choice for the dissipative and random force coefficients are $\gamma = 4.5$ and $\sigma = 3$.

Given the DPD equations of motion in this form, transport equations for the mass and momentum density fields have been analytically derived by Español[138] that, as expected, have the form of Navier–Stokes equations. In addition, in the same paper Español derives expressions for the pressure, and bulk and shear viscosities, for a system governed by the DPD equations of motion. Observing the form of the equations of motion under the DPD thermostat we see that there is a very elegant direct intuitive correspondence to the actual dynamics of a mesoscopic system. Since each DPD particle is composed of several atoms it can be seen itself as a subsystem with its own degrees of freedom. The dissipative and random forces thus represent transfer of energy between the internal and external degrees of freedom occurring in collisions with other particles, and one no longer has to postulate the system of particles being connected to an external heat bath.

1 Derivation of effective dissipative and random "forces" for algorithm with timestep Δt. Given the random impulse $\dot{W}_{ij}$ and finite timestep Δt, each ΔW_{ij} will be a random number chosen from a Gaussian distribution with variance Δt and zero mean, with the restrictions of $\Delta W_{ij} = \Delta W_{ji}$ and time reversibility. In the limit of large number of steps and small timestep, which we can safely assume for any realistic DPD algorithm, the central limit theorem permits us to replace the set of Gaussian random numbers of zero mean and variance Δt by a set of random numbers chosen from a uniform distribution with zero mean and variance $12\Delta t$, thus considerably reducing the computational overhead.[183]

$$\dot{W}_{ij} \approx \sqrt{12\Delta t}(\theta_{ij} - 0.5), \tag{4.13}$$

where θ_{ij} is a uniform random number on the range (0,1) and $\theta_{ij} = \theta_{ji}$. Thus given the above approximation and the parameter relations determined by Español and Warren (4.12), we have the following equations for the dissipative force and effective "random force" acting on each particle, for time step Δt given by:

$$\mathbf{F}_i^D = -\gamma \sum_{i \neq j} \omega_R(r_{ij})^2 (\dot{\mathbf{r}}_{ij} \cdot \hat{\mathbf{r}}_{ij}) \hat{\mathbf{r}}_{ij} \tag{4.14}$$

$$\mathbf{F}_i^R = \sqrt{\frac{24\gamma k_B T}{\Delta t}} \sum_{i \neq j} \omega_R(r_{ij}) \hat{\mathbf{r}}_{ij} (\theta_{ij} - 0.5) \tag{4.15}$$

2 Uncoupling the dissipative force. The standard algorithm that can be used to solve the equations of motion, while obeying time reversibility as specified by the Wiener process is the velocity-Verlet (VV) algorithm, which performs a second order splitting between the velocity and position degrees of freedom:

1. $\dot{\mathbf{r}}_i = \dot{\mathbf{r}}_i + \frac{\Delta t}{2m_i}(F_i^C + F_i^R + F_i^D)$
2. $\mathbf{r}_i = \mathbf{r}_i + \dot{\mathbf{r}}_i \Delta t$
3. calculate $F_i^C(\mathbf{r}_i)$, $F_i^R(\mathbf{r}_i)$ and $F_i^D(\mathbf{r}_i, \dot{\mathbf{r}}_i)$
4. $\dot{\mathbf{r}}_i = \dot{\mathbf{r}}_i + \frac{\Delta t}{2m_i}(F_i^C + F_i^R + F_i^D)$

It should be noted that, unlike the references where the DPD algorithm has been formulated, we explicitly include the masses of the individual particles.

The key complicating factor in the development of a numerical algorithm to solve the DPD equations of motion is the fact that the dissipative force is simultaneously coupled to the relative velocities and positions of the interacting particle pairs. As a result the standard time reversible numerical algorithms to solve the equations of motion with a finite small timestep Δt, the velocity-Verlet (VV) and leap frog algorithms, which perform a splitting between the position and velocity updates, break down. The first workable algorithm to solve the DPD equations of motion was developed by Groot and Warren.[129] The algorithm (GW) is a modification of the VV algorithm, where all the forces, like in VV, are only modified once per timestep, however the dissipative forces are modified based on intermediate "predicted" velocities, evaluated at a timestep determined by a phenomenological parameter λ. The GW algorithm consists of the following steps:

1. $\dot{\mathbf{r}}_i = \dot{\mathbf{r}}_i + \frac{\Delta t}{2m_i}(F_i^{\mathrm{C}} + F_i^{\mathrm{R}} + F_i^{\mathrm{D}})$
2. $\tilde{\mathbf{r}}_i = \dot{\mathbf{r}}_i + \lambda\frac{\Delta}{m_i}t(F_i^{\mathrm{C}} + F_i^{\mathrm{R}} + F_i^{\mathrm{D}})$
3. $\mathbf{r}_i = \mathbf{r}_i + \tilde{\mathbf{r}}_i\Delta t$
4. calculate $F_i^{\mathrm{C}}(\mathbf{r}_i)$, $F_i^{\mathrm{R}}(\mathbf{r}_i)$ and $F_i^{\mathrm{D}}(\mathbf{r}_i, \tilde{\mathbf{r}}_i)$
5. $\dot{\mathbf{r}}_i = \dot{\mathbf{r}}_i + \frac{\Delta t}{2m_i}(F_i^{\mathrm{C}} + F_i^{\mathrm{R}} + F_i^{\mathrm{D}})$

Clearly setting $\lambda = 1/2$ recovers the original VV algorithm. Groot and Warren found that this algorithm is optimized by setting $\lambda = 0.65$. While this algorithm was found to work, and is actually relatively efficient,[184] the fact that it contains a phenomenological parameter complicates how it can be predicted to behave when applied to new systems, as DPD is further developed. Several algorithms have been developed attempting to improve on the GW algorithm, that do not make use of a phenomenological parameter. These include the OC algorithm developed by Otter and Clarke,[185] the S1 algorithm, a symplectic Trotter decomposition scheme, developed by Shardlow,[186] the DPD-VV algorithm developed by Besold *et al.*,[187] and the self consistent velocity-Verlet algorithm, (SC-VV), of Paganobarraga and Frenkel.[188] All these algorithms, along with GW were tested and benchmarked by Nikunen *et al.*[189] Of these algorithms, OC was found to be sub-optimal, and while SC-VV performed very well, the self consistent renormalization of the temperature that is a part of the algorithm creates new problems that make this algorithm more trouble than it is worth.

The two algorithms which rate detailed description are the DPD-VV which is trivial to implement, has an acceptable accuracy in the appropriate time step range of the algorithm ($\Delta t \approx 0.05$ in reduced units), and has been thoroughly tested, and the S1 algorithm which preserves conserved quantities better than the DPD-VV, has not been as widely used, and is not as trivial (though not so incredibly difficult) to implement as the DPD-VV algorithm. A very recent development is a generalization of the Trotter integration scheme used by Shardlow, proposed by Serrano *et al.*[190]

The DPD-VV algorithm is simply the VV algorithm with the dissipative force recalculated on the half timestep:

1. $\dot{\mathbf{r}}_i = \dot{\mathbf{r}}_i + \frac{\Delta t}{2m_i}(F_i^{\mathrm{C}} + F_i^{\mathrm{R}} + F_i^{\mathrm{D}})$
2. $\mathbf{r}_i = \mathbf{r}_i + \dot{\mathbf{r}}_i\Delta t$
3. calculate $F_i^{\mathrm{C}}(\mathbf{r}_i)$, $F_i^{\mathrm{R}}(\mathbf{r}_i)$ and $F_i^{\mathrm{D}}(\mathbf{r}_i, \dot{\mathbf{r}}_i)$
4. $\dot{\mathbf{r}}_i = \dot{\mathbf{r}}_i + \frac{\Delta t}{2m_i}(F_i^{\mathrm{C}} + F_i^{\mathrm{R}} + F_i^{\mathrm{D}})$
5. calculate $F_i^{\mathrm{D}}(\mathbf{r}_i, \dot{\mathbf{r}}_i)$

The S1 algorithm involves performing a Trotter first order splitting of the velocity-Verlet algorithm between the effect of the random and dissipative forces, and the effect of the conservative force. In the resulting algorithm each timestep contains a constant energy VV step alongside an extra step where the particle velocities are updated due to the effects of the dissipative and random forces, as follows:

If we consider:

$$\mathbf{f}_{ij}^{D} = -\gamma\omega_{\mathrm{R}}(r_{ij})^2(\hat{\mathbf{r}}_{ij}\cdot\dot{\mathbf{r}}_{ij})\hat{\mathbf{r}}_{ij} \tag{4.16}$$

$$\mathbf{f}_{ij}^{\mathrm{R}} = \sqrt{\frac{24\gamma k_{\mathrm{B}}T}{\Delta t}}\omega_{\mathrm{R}}(r_{ij})\,\hat{\mathbf{r}}_{ij}(\theta_{ij} - 0.5) \tag{4.17}$$

$$\mathbf{s}_{ij}^{\mathrm{D}} = -\frac{1}{1 + \gamma\omega_{\mathrm{R}}(r_{ij})^2\Delta t} \tag{4.18}$$

$$\mathbf{s}_{ij}^{\mathrm{R}} = 1 - \frac{\gamma\omega_{\mathrm{R}}(r_{ij})^2\Delta t}{1 + \gamma\omega_{\mathrm{R}}(r_{ij})^2\Delta t} \tag{4.19}$$

for each interacting particle pair ij

(a) Calculate $\dot{\mathbf{r}}_{ij}$, $\mathbf{f}_{ij}^{\mathrm{D}}$, $\mathbf{f}_{ij}^{\mathrm{R}}$, $\mathbf{s}_{ij}^{\mathrm{D}}$ and $\mathbf{s}_{ij}^{\mathrm{R}}$,

(b) $\dot{\mathbf{r}}_i = \dot{\mathbf{r}}_i + \frac{\Delta t}{2m_i}(f_{ij}^{\mathrm{R}} + f_{ij}^{\mathrm{D}})$

$\dot{\mathbf{r}}_j = \dot{\mathbf{r}}_j - \frac{\Delta t}{2m_i}(f_{ij}^{\mathrm{R}} + f_{ij}^{\mathrm{D}})$

(c) Recalculate $\dot{\mathbf{r}}_{ij}$ and $\mathbf{f}_{ij}^{\mathrm{D}}$

(d) $\dot{\mathbf{r}}_i = \dot{\mathbf{r}}_i + \frac{\Delta t}{2m_i}(s_{ij}^{\mathrm{R}}f_{ij}^{\mathrm{R}} + s_{ij}^{\mathrm{D}}f_{ij}\mathrm{D})$

$\dot{\mathbf{r}}_i = \dot{\mathbf{r}}_i - \frac{\Delta t}{2m_i}(s_{ij}^{\mathrm{R}}f_{ij}^{\mathrm{R}} + s_{ij}^{\mathrm{D}}f_{ij}^{\mathrm{D}})$

2. $\dot{\mathbf{r}}_i = \dot{\mathbf{r}}_i + \frac{\Delta t}{2m_i}F_i^{\mathrm{C}}$
3. $\mathbf{r}_i = \mathbf{r}_i + \dot{\mathbf{r}}_i\Delta t$
4. calculate $F_i^{\mathrm{C}}(\dot{\mathbf{r}}_i)$
5. $\dot{\mathbf{r}}_i = \dot{\mathbf{r}}_i + \frac{\Delta t}{2m_i}F_i^{\mathrm{C}}$

3 Recent methodological developments of DPD. As stated previously the use of random and dissipative forces is not the only effective thermostat for DPD simulation. The methods of Lowe[162] and the extension of this method proposed by Stoyanov and Groot[163] propose a very different alternative. In the same way that the above described DPD algorithm takes Langevin dynamics as the starting point, the algorithm proposed by Lowe takes the Andersen thermostat as the starting point, hence the name by which it is commonly known, the "Lowe–Andersen" thermostat. In the same way that the Andersen thermostat makes stochastic adjustments directly to the velocities in the simulation, the Lowe–Andersen thermostat performs in a pairwise fashion thus conserving microscopic momentum. This algorithm performs extremely well, in many cases better than any other, when it has been benchmarked using standard conservation tests against existing DPD algorithms.[164,184,189] Thermalization is performed

collectively through a Monte Carlo process, with the probability of each individual particle pair being thermalized being controlled by the parameter in the algorithm Γ. Its use in MD simulations and influence on dynamic properties have been recently studied by Koopman and Lowe,[191] and it was shown to work well as long as the density of the system is reasonably large and the parameter Γ is not too high. For gaseous systems Koopman and Lowe recommend the algorithm of Stoyanov and Groot,[163] that hybridizes the Lowe–Andersen thermostat with what they claim is a momentum-conserving Nosé–Hoover algorithm. When looked at more closely the algorithm the Lowe–Andersen thermostat is hybridized with in actual fact bears closer resemblance to a momentum conserving Berendsen thermostat.[164] Since correct temperature fluctuations are not reproduced by the Berendsen thermostat the correctness of this algorithm is in doubt, and thus it needs further testing before it can be applied.

Two very exciting recent developments to the DPD algorithm have emerged from Jakobsen *et al.* The development of a multiple time step algorithm[192] promises, as it is further developed, to alleviate one of the main problems of DPD simulation, the inability to include important forces that act on shorter length and time scales, but effect the structure and dynamics on the mesoscale, without losing the advantages of DPD that allow for the observation of the longer length and time scales. They have also developed a new algorithm, described in explicit detail in ref. 193 that extends DPD-VV to allow DPD simulation to be performed in both constant pressure and constant surface tension, which has allowed for the simulation of biological membranes using DPD.[194] Thermostating also remains an active field, and the latest addition is the robust "extended DPD thermostat" by Junghans *et al.*[195]

4 Analytical approaches: regarding a systematic derivation of DPD. The standard DPD with soft potentials as presented above is phenomenological. An interesting formal approach has been presented by Flekkøy *et al.*[196,197] who were able to link DPD to molecular level properties by using a Voronoi tessellation-based technique. This method can be used to resolve different length scales simultaneously. The method is formally akin to the well-known renormalization group procedure extensively used in analytical treatment of critical phenomena.[25] The mathematical details can be found from the original articles as cited above.

The approach of Flekkøy *et al.* provides a systematic and computationally tractable, although not straightforward, method to coarse-grain molecular systems. From a computational point of view their method is more demanding than particle based methods such as the standard DPD as the Voronoi tessellation procedure, as it requires N log N operations and involves a fairly large additional prefactor.

V. Solvent free membranes

A Why do it?

So far we have discussed how one can proceed to coarse grain the simulation model, and the appropriate methodology to simulate the dynamics of systems using mesoscopic potentials. But as stated in the introduction, for most systems we still have the problem of the vast majority of our computational resources being used to simulate the solvent, in which the interesting system is immersed, interacting with itself. In this chapter we discuss simulation methods that do away with the solvent altogether.

Coarse graining is driven by the desire to reach larger length- and time scales. Let us illustrate that for membranes by asking: how does the effort to simulate a square patch of membrane of side length L scale with L? In the absence of embedding solvent the amount of material evidently increases with L^2, but there is a more severe limitation. It is not sufficient to *represent* a bilayer patch in the computer, it is necessary to also *equilibrate* it. Unfortunately, the equilibration time scales very unfavorably with L—in the absence of hydrodynamic interactions and at vanishing tension like L^4, owing to the nature of the underlying curvature-elastic Hamiltonian. Thus, the entire effort scales like L^6. Extending the simulation of a fully equilibrated 20 nm bilayer,[198] big enough to answer localized questions, to maybe 200 nm, possibly necessary to study cooperative interaction and aggregation behavior of membrane proteins, we need a million times more computer time.

We have seen in this review that a variety of different techniques and models have been developed to coarse-grain lipids and membranes. But when one arrives at these large scales, there often is yet another effect which works against us: membranes begin to significantly bend. By ceasing to be essentially flat, the volume of the simulation box is no longer given by L^2b, where b is equal to the bilayer thickness plus a hydration layer, but rather begins to scale like L^3 (think for instance of simulating a vesicle). The ratio between material and box-volume decreases like L^{-1}, exactly as if one were for instance simulating a Gaussian polymer coil. And just as in the polymer case the evident solution is to eliminate the solvent in favor of effective interactions. Unlike in the polymer case, however, the way to achieve this turns out to be a bit more tricky.

B Basic ideas and specific implementations

The self-assembly of a lipid bilayer is driven by the hydrophobic effect created by the solvent, so eliminating the solvent requires us to mimic the hydrophobic effect by some effective cohesion potential. Unlike polymers, held together by chemical bonds, the structural integrity of the bilayer aggregate depends on this cohesion energy, so its form will matter. In past research it has been found that a simple short ranged (*e.g.* Lennard-Jones like) attractive interaction between coarse-grained hydrophobic lipid chains will not usually work. Such interactions have been found not to be able to to produce aggregates which were both bilayer-like and fluid (for a short discussion see ref. 199). The issue is that aggregation from a 3D lipid distribution into a 2D aggregate seems to require a binding strength which is incompatible with a fluid condensed phase. In order to overcome this obstacle, various solutions have been proposed:

1 Multibody potentials. Performing a partial trace over selected degrees of freedom in the partition function results in new effective interactions between the remaining ones which, however, do not necessarily have to be of equally

simple type as the original interactions (*e.g.* pair-wise). Indeed, Drouffe *et al.*, who first successfully managed to aggregate a fluid membrane under solvent-free conditions, implemented a multibody-potential between its highly coarse-grained amphiphiles.[200] The latter were chosen to be spherical polar beads with three interactions between them: (A) a hard core repulsion; (B) a dipolar-like attraction favoring planar alignment; and (C) a density-dependent cohesion which prefers each bead to have 6 neighbors. This model was able to spontaneously aggregate into two-dimensional sheets which, due to line tension, closed to form vesicles. An analysis of the shape fluctuation yielded a bending modulus $\kappa \approx 3k_BT$.

Ten years later Noguchi and Takasu picked up this concept and extended it to slightly less coarse-grained amphiphiles, modeled as a rigid linear array of three connected beads, two of them "hydrophobic".[201,202] In this case the cohesive interaction $U(\rho)$ is chosen to depend on the local (somewhat smoothed) particle density ρ in such a way that it is proportional to ρ at sufficiently small ρ, but levels off beyond a certain limit, according to

$$\rho_{i,j} = \sum_{i \neq i',j'=2,3} h(|\mathbf{r}_{i,j} - \mathbf{r}_{i',j'}|) \tag{5.1a}$$

$$h(r) = 1/\{\exp[20(r/\sigma - 1.9)] + 1\} \tag{5.1b}$$

$$U(\rho) = \begin{cases} -0.5\rho, & \rho < \rho^* - 1 \\ 0.25(\rho - \rho^*)^2 - c, & \rho^* - 1 \leq \rho < \rho^* \\ -c, & \rho^* \leq \rho \end{cases} \tag{5.1c}$$

where i, i' numbers the lipids, j, $j' = 2,3$ the two hydrophobic tail beads, $\rho^* = 10$ and $c = 4.75$ for $j = 2$ and $\rho^* = 14$ and $c = 6.75$ for $j = 3$, and where σ is the bead diameter. Notice that for small densities this just reduces to a pair attraction $h(r)$, while as the density increases during self-assembly, this leveling off prevents too strong attractions which might drive the system right away into the gel phase. With these system bending rigidities of $\kappa/k_BT = 1\ldots5$ were found.[202]

A few years later Wang and Frenkel proposed a variant of this model,[203] in which the lipids had an additional bending degree of freedom and the density dependence of the hydrophobic interactions was parametrized slightly differently, in particular by evaluating the average density of hydrophobic units inside a slightly prolate ellipsoid, oriented along the direction of the average bilayer normal. Within their parametrization these authors obtained a physically more realistic bending rigidity of $\kappa/k_BT \approx 13$, as measured *via* a fluctuation analysis.

2 Orientational dependencies. Even though the use of multibody potentials led to solvent free models which showed robust self-assembly, such potentials are usually more difficult to manage than ordinary pair potentials. Their implementation in "standard" packages might be more difficult, the calculation of observables such as the stress tensor is more involved, and some of the statistical mechanical intuition based on our habitual use of pair potentials is inapplicable. For this reason people have strived to make a pure pair approach work. One suggestion by Brannigan and Brown was based on the use of an orientation dependent cohesive force.[204] Using spherocylinders as the shape of their lipids, they introduced orientation dependent alignment and cohesion interactions in the form

$$U_{\text{align}}(\boldsymbol{r}_{ij}, \hat{\boldsymbol{n}}_i, \hat{\boldsymbol{n}}_j) = -c_{\text{align}} \left(\frac{\sigma}{|r_{ij}|}\right)^2 \frac{\sin^2\theta_i + \sin^2\theta_j}{2}, \tag{5.2a}$$

$$U_{\text{cohesion}}(\boldsymbol{r}_{ij}, \hat{\boldsymbol{n}}_i, \hat{\boldsymbol{n}}_j) = -c_{\text{cohesion}} \left(\frac{\sigma}{|\boldsymbol{r}_{ij} + \lambda(\hat{\boldsymbol{n}}_j - \hat{\boldsymbol{n}}_i)|}\right)^6, \tag{5.2b}$$

where $\hat{n}_i$ is the unit vector pointing in the direction of the long axis of lipid i, θ_i and θ_j are the angles between the lipid axis of lipids i and j and their separation vector $\boldsymbol{r}_{ij}$, and λ is the length of the spherocylinder (without the two caps). The potentials U_{align} and U_{cohesion} are cut off and shifted to zero at $r = 3\sigma$ and $r = 2\sigma$, respectively, and the values of the two coupling constants c_{align} and c_{cohesion} were systematically varied. Additionally, an excluded volume repulsion of the form $U_{\text{core}}(d_{ij}) = c_{\text{core}}(\sigma/d_{ij})^8$ was included, where d_{ij} is the distance of closest approach between the two spherocylinders i and j.

The resulting phase diagram contained regions of fluid bilayers, with relatively high bending rigidities in the range $\kappa/k_BT = 60\ldots120$. However, self assembly could only be achieved by artificially guiding the emerging aggregates toward equilibrium, namely, by beginning in a warm dense simulation box and ending up in a cold dilute one.

3 Highly tuned individual interactions. Farago has shown that it is possible to completely revert to pair potentials of Lennard-Jones $(n,2n)$-type, provided they are very carefully parametrized.[205] He uses again a rigid HTT-trimer and tunes the interactions between individual beads (HH, HT_1, HT_2, T_1T_1, T_1T_2, T_2T_2) in strength, range, and functional form (for details see ref. 205). One can thus stabilize a fluid phase, and he measures a bending rigidity around $\kappa/k_BT \simeq 50$. Unfortunately the effort going into the tuning of all these potentials makes it difficult to systematically vary membrane parameters (such as rigidity or order) without essentially reparametrizing all of them together.

4 Longer ranged attractions. An easier way to revert to pair forces is the use of cohesive interactions that are sufficiently long ranged. The Farago model already hinted towards the advantage of having cohesive interactions extend over a range longer than the typical Lennard-Jones (6,12) distance. Two models have been proposed recently, which owe their success essentially to a systematic exploitation of this effect. The first is due to Brannigan, Philips and Brown,[206] who use a 5-bead lipid of composition "HITTT" (one head-bead, one interface bead and three tail beads) with the following interactions

$$U_{\text{core}}(r) = c_{\text{core}}(\sigma/r)^{12} \ (r_{\text{cut}} = 2\sigma), \tag{5.3a}$$

$$U_{\text{tail}}(r) = -c_{\text{tail}}(\sigma/r)^6 \ (r_{\text{cut}} = 2\sigma), \tag{5.3b}$$

$$U_{\text{int}}(r) = -c_{\text{int}}(\sigma/r)^2 \ (r_{\text{cut}} = 3\sigma), \tag{5.3c}$$

where U_{core} acts between all beads except intramolecular bead pairs separated by less than three bonds, U_{tail} acts between all TI and TT pairs, and U_{int} between all II pairs; all potentials are cut-off and shifted to zero at the indicated distance. The

rationale for additional long ranged interfacial attraction stems from the fact that it is precisely on the hydrophilic/hydrophobic interface between the lipid heads and tails where the cohesive stress is localized. The chosen parameters are $c_{core} = 0.4\varepsilon$, $c_{tail} = 1.0\varepsilon$, $c_{int} = 3.0\varepsilon$, where ε is the unit of energy. Additionally, a bending term of the form $c_{bend} \cos\theta$ between any three successive beads is implemented, and the lipid bending stiffness c_{bend} is varied between 5ε and 10ε. Corresponding membrane bending rigidities vary in the range $\kappa/k_BT = 2.5\ldots16$.

The second model, due to Cooke, Kremer and Deserno,[207] uses again a semiflexible lipid trimer of the form "HTT" with the following interactions:

$$U_{bond}(r) = \tfrac{1}{2}k_{bond}r_\infty^2 \ln[1 - (r/r_\infty)^2], \quad (5.4a)$$

$$U_{core}(r,b) = 4\varepsilon\left[\left(\frac{b}{r}\right)^{12} - \left(\frac{b}{r}\right)^{6}\right], \ (r_{cut} = 2^{1/6}b), \quad (5.4b)$$

$$U_{attr}(r,w_c) = \begin{cases} -\varepsilon, & r < r_c \\ -\varepsilon\cos^2\frac{\pi(r-r_c)}{2w_c}, & r_c < r < r_c + w_c \end{cases}, \quad (5.4c)$$

with $k_{bond} = 30\varepsilon$ and $r_\infty = 1.5\sigma$. Additionally, the lipid is straightened by a pseudo bending potential between the head-bead and the second tail bead of the form $\frac{1}{2}k_{bend}(r_{HT2} - 4\sigma)^2$ with $k_{bend} = 10\varepsilon/\sigma^2$. All beads interact repulsively with $U_{core}(r,b)$, where $b_{HH} = b_{HT} = 0.95\sigma$ and $b_{TT} = \sigma$ to ensure a cylindrical shape. The cohesive potential $U_{attr}(r,w_c)$ acts only between tail-beads. Its range w_c can be tuned. If it is too short ($w_c \lesssim 0.75\sigma$) lipids either do not aggregate or assemble into a gel phase, while for larger w_c a fluid phase emerges within some temperature range. In this range a fluctuation analysis shows that bending rigidities in the range $\kappa/k_BT = 3\ldots30$ can be reached.

C Example applications

The models described above are highly coarse grained, both in terms of a substantially reduced number of degrees of freedom and because the solvent has been eliminated. Yet, many relevant insights can be gained from them, since one can both achieve excellent statistics in static questions and large time scales in dynamic ones. In the following we would like to present a short list of examples which illustrate the potential of this coarse-graining approach.

1 Elastic moduli from shape fluctuations. Bilayer membranes show constant thermal fluctuations. It is well known that in the continuum limit the mean squared Fourier modes of an asymptotically flat membrane decay like $k_BT/(\kappa q^4 + \sigma q^2)$, where q is the wave vector and κ and σ are bending modulus and lateral tension, respectively. Recently Brannigan and Brown have pointed out that a careful analysis of the complete shape fluctuations—including undulation and peristaltic modes—gives access to other highly relevant observables, most notably the spontaneous monolayer curvature.[208] They derive analytical expressions for the fluctuation spectrum at all values of q, up to the protrusion regime, and show that it can be fit very well to both atomistic simulations and their coarse-grained model which we briefly described in section VB4. Not only validating the physics which entered their coarse-graining scheme, it also suggests a clear route for parameter optimization, if one intends to match specific lipid systems.

Efficient sampling of the long wave length undulations, the ones most relevant for determining the bending modulus, is often hampered by their slow equilibration time, which is proportional to the fourth power of their wave length in the solvent free case. Farago has recently shown that this limitation can be elegantly overcome by additional Monte Carlo moves.[209] Large scale shape changes are effected by imprinting undulation modes with the correct expected amplitude onto the membrane and accept such reshaped configurations according to the usual Metropolis criterion. For a system of 9000 lipids (and a model very similar to the Cooke model from section VB4) a speed-up by a factor of 50 has been measured compared to single particle Monte Carlo moves.

2 Bending rigidity *via* tether pulling. While the membrane bending modulus κ is accessible from thermal fluctuations, this technique displays two limitations: first, it becomes difficult for fairly stiff membranes to resolve the small amplitude fluctuations; and second, it invariably only probes very weak (thermally excited) curvatures, leaving open the question whether quadratic bending elasticity remains a faithful description at high bending. Harmandaris and Deserno have recently shown that the bending rigidity can alternatively be obtained from simulating cylindrical membrane tethers, since (up to subdominant fluctuations) $\kappa = FR/2\pi$, where F is the tensile force required to hold a bilayer tether of radius R,[210] see Fig. 7 for an illustration. Using the Cooke model described in section VB4 and the ESPResSo simulation package[211] they showed that this measurement of κ coincides with the one obtained from thermal fluctuations up to curvature radii comparable to bilayer thickness. This method is also particularly suitable for solvent free systems, since: (i) non-flat bilayers are essential; and (ii) no complications arise from the fact that the

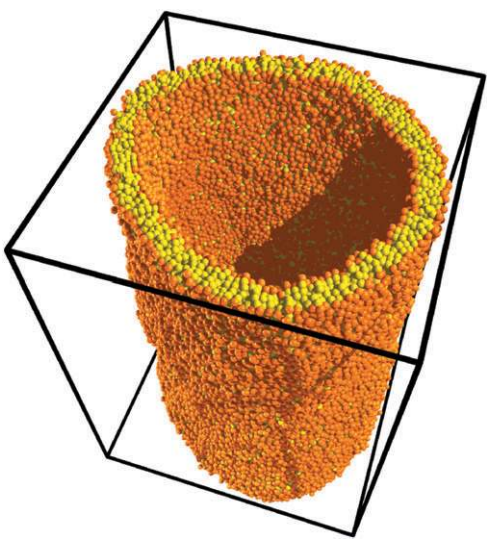

Fig. 7 Simulation of a cylindrically shaped membrane tether. Notice that due to periodic boundary conditions the tether has no open edges. Curvature stresses result in an axial tensile force of magnitude $F = 2\pi\kappa/R$, from which the bending modulus κ can be easily extracted.[210]

cylinder separates two different compartments (inside and outside) whose pressure difference otherwise would need to be relaxed by transporting solvent.

The same idea (in a slightly different implementation) has recently been applied by Arkhipov *et al.* to a different solvent free CG lipid model.[212] These authors also find that within the obtained accuracy the measured bending modulus does not depend on tether radius.

3 Lipoplexes. When cationic membranes (consisting of a mixture of cationic and neutral lipids) are brought in contact with DNA, they form complexes called "lipoplexes" in which parallel DNA strands are sandwiched between lipid bilayers. Their cohesive energy is thus driven by a combination of electrostatic interactions (ultimately counterion release entropy) and the hydrophobic interactions between lipid tails. Farago *et al.* have recently studied this complexation behavior at isoelectric mixing, using the coarse-grained model discussed in section VB3.[213,214] Due to the simplicity of the model, equilibrated complexes containing up to $N = 1000$ lipids (a fraction ϕ_c of which was charged) could be studied. In particular, the experimentally observed scaling $d_{DNA} \sim \phi_c^{-1}$ could be confirmed, and it was shown that at large ϕ_c the electrostatically induced stress can lead to local pore opening of the bilayer phases.

4 Curvature-mediated interactions. Membranes can adsorb particles at their surface, such as, for instance, peripheral membrane proteins. It is known that such proteins might locally induce quite substantial membrane deformations, as has recently been vividly illustrated in atomistic simulations of N-BAR domains.[216] What happens, if many such membrane benders have a chance to cooperatively affect the membrane shape? The exciting possibility one might want to explore is whether they could aggregate and induce a large curved membrane bud. But if so, we immediately see that there is very little chance to study this problem at high resolution, since membrane extensions in the 100-nanometer range are required, and timescales maybe up to a millisecond. Moreover, if budding really sets in, the initially flat membrane bulges out and calls for a genuinely three-dimensional simulation box, which becomes extremely costly if solvent is present. These initial thoughts show that a problem of this kind suggests very strongly the use of a coarse-grained solvent-free approach. Indeed, Reynwar *et al.* have recently performed such a simulation, using the Cooke model described in section VB4[215] and the ESPResSo simulation package.[211] They have demonstrated that sufficiently many curved proteins, each imposing a sufficient curvature, can indeed lead to the formation of a membrane bud. For extremely strong membrane deformers, such as partially adhering viral capsids (see Fig. 8), they also demonstrated the existence of attractive pair forces.

Using a much a more highly coarse-grained description of a membrane as a triangulated surface, and accounting for the presence of N-BAR domains by locally imposing a nonzero curvature tensor, Ayton *et al.* have also shown that membranes studded with curvature-imprinting proteins spontaneously form tubules and highly curved structures.[217]

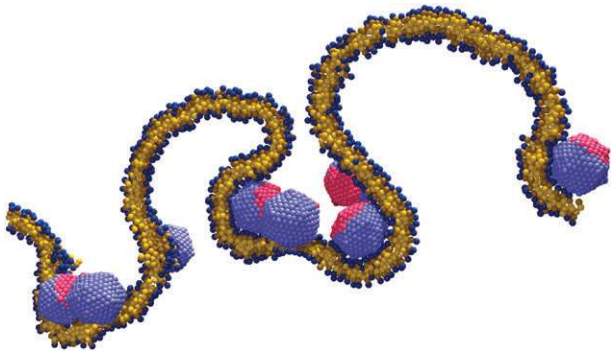

Fig. 8 Slice through a large membrane studded with partially adhesive spheres. These spheres wrap themselves to about $\frac{3}{4}$ inside the membrane, but cannot completely get covered and thus not "bud" off from the membrane. However, membrane mediated interactions lead to the attraction of several such local membrane benders, which by driving a large morphology change can then cooperatively create a joint budding vesicle. For instance, the highly bent structure in the middle will detach from the membrane through a fission event within the next 30 μs.[215]

Moreover, Arkhipov *et al.* have recently studied the effectivity with which many N-BAR domains can curve an initially flat bilayer patch[212] using a multiscaling study bridging four scales: from atomistic simulations, over residue- and shape-based coarse-graining up to continuum elasticity.

VI. Summary

In this article, we have focused on four issues: first, using structural information from atomistic or detailed models (or experiments) to construct coarse-grained models in a hierarchical and systematic way. Our approach is based on the Henderson theorem (section IIA) and the Inverse Monte Carlo method of Lyubartsev and Laaksonen (section IIC) which was then extended by the use of a thermodynamic constraint (section IID). Second, we took a different look at coarse graining by analyzing conformations of molecules. This was done by the application of self-organizing maps. Third, we discussed the dissipative particle dynamics (DPD) method in section IV. The focus was on technical issues and integration of the equations of motion. The final, and fourth, topic was solvent free modeling (section V) which offers a different route to coarse graining by integrating out the degrees of freedom associated with solvent.

The field of multiscale modeling is very active and both conceptual and technical matters are under rapid development. It is impossible to cover all aspects (or even most) in one review. To finish this review, we wish to give the reader a few pointers to the issues we did not cover here. First, we neglected matters related to electrostatics, yet it is one of the most important issues in simulations of biological and soft matter. There have been some new developments especially by Groot[218,219] with regard to DPD and Voth *et al.*[220] in terms of more general coarse-grained systems. The recent review of Karttunen *et al.*[221] covers some general aspects and new methods related to electrostatics. We also neglected field theoretical models. There have been several interesting

developments, especially the recent work of Haataja *et al.*[222] related to lipid rafts.

Software and parameters for multiscale simulations in soft and biological matter

Here we provide a short list of free software, parameters (GPL or comparable license) and the related web sites as they may be useful for the reader. We make no attempt to evaluate the software or parameters as that is beyond the scope of this review. We encourage the interested reader to take a look at the sites and also to contribute him/herself. The list is not exhaustive but rather based on our own personal experience.

We would also like to point out there is currently a lot of activity in software development. For example, smart middleware such as Charm++[223] have helped in parallelization of MD simulations to 1000s of processors, and new approaches using graphics cards[224,225] seem very promising.

- Espresso:[211] http://www.espresso.mpg.de/
- Lampps:[226] http://lammps.sandia.gov
- Gromacs:[227] http://www.gromacs.org
- Parameters: http://moose.bio.ucalgary.ca/index.php?page=Downloads
- NAMD2[228,229] and VMD:[230] http://www.ks.uiuc.edu/Development/
- Softsimu[26] software, DPD with bond crossing constraints[145] and parameters: http://www.softsimu.org/downloads.shtml
- MDynaMix:[231] http://www.fos.su.se/~sasha/md_prog.html
- DL_POLY: http://www.cse.scitech.ac.uk/ccg/software/DL_POLY/
- OCTA:[232] http://octa.jp/

Acknowledgements

We would like to thank our students, postdocs and co-workers with whom a lot of the work reviewed here has been conducted, in particular Petri Nikunen, Emma Falck, Michael Patra, Andrea Catte, Aatto Laaksonen, Alexander Lyubartsev, James Polson, Gerhard Besold, Ira Cooke, Ben Reynwar, Gregoria Illya, Vagelis Harmandaris, Christian Holm and Kurt Kremer.

This work has been supported by the Natural Sciences and Engineering Research Council of Canada (M. K.) and the German Science Foundation (M. D.). We also thank the Southern Ontario SharcNet (http://www.sharcnet.ca) computing facility, the Distributed European Infrastructure for Supercomputing Applications (http://www.deisa.eu) and the Finnish IT Centre for Science for computer resources.

References

1 R. P. Feynman, R. B. Leighton and M. Sands, *The Feynman Lectures on Physics*, Addison-Wesley, Reading, MA, 3rd edn, 1963, vol. I.
2 M. Chaplin, *Nat. Rev. Mol. Cell Biol.*, 2006, **7**, 861.
3 A. R. Fresht, *Nat. Rev. Mol. Cell Biol.*, 2008, **9**, 650.
4 C. Branden and J. Tooze, *Introduction to Protein Strcuture*, Garland, New York, NY, 2nd edn, 1999.
5 B. Mergell, R. Everaers and H. Schiessel, *Phys. Rev. E: Stat., Nonlinear, Soft Matter Phys.*, 2004, **70**, 011915.
6 J. Langowski and H. Schiessel, *New Comp. Biochem.*, 2004, **39**, 397.
7 H. Schiessel, *J. Phys.: Condens. Matter*, 2003, **15**, R699.
8 D. L. Nelson and M. M. Cox, *Lehninger Principles of Biochemistry*, W. H. Freeman, 5th edn, 2008.
9 *Soft Matter Physics*, ed. M. Daoud and C. E. W, Springer-Verlag, Berlin, 1999.
10 *Physics of Biological Systems: From Molecules to Species*, ed. H. Flyvjberg, J. Hertz, M. H. Jensen, O. G. Mouritsen and K. Sneppen, Springer-Verlag, Berlin, 1997.
11 *Soft and Fragile Matter: Nonequilibrium Dynamics, Metastability and Flow*, ed. M. E. Cates and M. R. Evans, Institute of Physics Publishing, Bristol, 2000.
12 B. Alberts, D. Bray, J. Lewis, M. Raff, K. Roberts and J. D. Watson, *Molecular Biology of the Cell*, Garland Publishing, New York, 3rd edn, 1994.
13 T. Schlick, *Molecular Modeling and Simulation*, Springer-Verlag, New York, 2002.
14 H. W. Kroto, *Nobel lecture*, 1996.
15 D. Frenkel and B. Smit, *Understanding Molecular Simulation: From Algorithms to Applications*, Academic Press, San Diego, 2nd edn, 2002.
16 M. P. Allen and D. J. Tildesley, *Computer Simulation of Liquids*, Clarendon Press, Oxford, 1987.
17 A. R. Leach, *Molecular Modelling: Principles and Applications*, Prentice Hall, Harlow, 2001.
18 S. J. Marrink, A. H. de Vries and A. E. Mark, *J. Phys. Chem. B*, 2004, **108**, 750.
19 S. J. Marrink, H. J. Risselada, S. Yefimov, D. P. Tieleman and A. H. de Vries, *J. Phys. Chem. B*, 2007, **111**, 7812.
20 L. Monticelli, S. K. Kandasamy, X. Periole, R. G. Larson, D. P. Tieleman and S.-J. Marrink, *J. Chem. Theory Comput.*, 2008, **4**, 819.
21 S. J. A. Van Ginsbergen, J. G. Snijders and E. J. Baerends, *J. Chem. Phys.*, 1995, **103**, 9347.
22 C. Y. Yam, S. Yokojima and G. Chen, *J. Chem. Phys.*, 2003, **119**, 8794.
23 P. S. Niemelä, S. Ollila, M. T. Hyvönen, M. Karttunen and I. Vattulainen, *PLoS Comput. Biol.*, 2007, **3**, 0304.
24 A. Arkhipov, P. L. Freddolino and K. Schulten, *Structure*, 2006, **14**, 1767.
25 N. Goldenfeld, *Lectures on Phase Transitions and the Renormalization Group*, Addison-Wesley, Reading, MA, 1992.
26 *Novel Methods in Soft Matter Simulations*, ed. M. Karttunen, I. Vattulainen and A. Lukkarinen, Lecture Notes in Physics, Springer Verlag, Heidelberg, 2004.
27 M. Müller, K. Katsov and M. Schick, *Phys. Rep.*, 2006, **434**, 113.
28 M. Venturoli, M. M. Sperotto, M. Kranenburg and B. Smit, *Phys. Rep.*, 2006, **437**, 1.
29 *Computational Modeling of Membrane Bilayers*, ed. S. K. Feller, Elsevier, Amsterdam, 2008, vol. 60.
30 *Coarse-Graining of Condensed Phase and Biomolecular Systems*, ed. G. Voth, CRC Press, Boca Raton, FL, 2008.
31 M. Praprotnik, L. Delle Site and K. Kremer, *Annu. Rev. Phys. Chem.*, 2008, **59**, 545.
32 A. Catte, J. C. Patterson, D. Bashtovyy, M. K. Jones, F. Gu, L. Li, A. Rampioni, D. Sengupta, T. Vuorela, P. Niemelä, M. Karttunen, S. J. Marrink, I. Vattulainen and J. P. Segrest, *Biophys. J.*, 2008, **94**, 2306.
33 R. Zwanzig, *J. Chem. Phys.*, 1960, **33**, 1338.
34 H. Mori, *Prog. Theor. Phys.*, 1965, **33**, 423.
35 R. L. C. Akkermans and W. J. Briels, *J. Chem. Phys.*, 2000, **113**, 6409.
36 M. Grmela and H. C. Öttinger, *Phys. Rev. E*, 1997, **56**, 6620.
37 M. Grmela and H. C. Öttinger, *Phys. Rev. E*, 1997, **56**, 6633.
38 H. C. Öttinger, *Phys. Rev. E*, 1998, **57**, 1416.
39 S. Majaniemi and M. Grant, *Phys. Rev. B: Condens. Matter Mater. Phys.*, 2007, **75**.
40 J.-P. Hansen and I. R. McDonald, *Theory of Simple Liquids*, Academic Press, San Diego, CA, 2nd edn, 1990.
41 P. G. Bolhuis, A. A. Louis, J.-P. Hansen and E. Meijer, *J. Chem. Phys.*, 2001, **114**, 4296.
42 A. A. Louis, P. Bolhuis, J.-P. Hansen and E. Meijer, *Phys. Rev. Lett.*, 2000, **82**, 2522.

43 L. Reatto, D. Levesque and J. J. Weis, *Phys. Rev. A*, 1986, **33**, 3451.
44 Y. Rosenfeld and G. Kahl, *J. Phys.: Condens. Matter*, 1997, **9**, L89.
45 P. Gonzalez-Mozuelos and M. D. Carbajal-Tinoco, *J. Chem. Phys.*, 1998, **24**, 11074.
46 A. P. Lyubartsev and S. Marcelja, *Phys. Rev. E: Stat., Nonlinear, Soft Matter Phys.*, 2002, **65**, 041202.
47 S. Chen and G. D. Doolen, *Annu. Rev. Fluid Mech.*, 1998, **30**, 329.
48 A. Malevanets and R. Kapral, *J. Phys. Chem.*, 1999, **110**, 8605.
49 A. Malevanets and R. Kapral, *J. Chem. Phys.*, 2000, **112**, 7260.
50 A. Malevanets and J. M. Yeomans, *Europhys. Lett.*, 2000, **52**, 231.
51 N. Kikuchi, A. Gent and J. M. Yeomans, *Eur. Phys. J. C*, 2002, **E9**, 63.
52 T. Ihle and D. M. Kroll, *Phys. Rev. E: Stat., Nonlinear, Soft Matter Phys.*, 2001, **63**, 020201.
53 T. Ihle and D. M. Kroll, *Phys. Rev. E: Stat., Nonlinear, Soft Matter Phys.*, 2003, **67**, 066705.
54 T. Ihle and D. M. Kroll, *Phys. Rev. E: Stat., Nonlinear, Soft Matter Phys.*, 2003, **67**, 066706.
55 E. Tüzel, M. Strauss, T. Ihle and D. M. Kroll, *Phys. Rev. E: Stat., Nonlinear, Soft Matter Phys.*, 2003, **68**, 036701.
56 A. Lamura and G. Gompper, *Eur. Phys. J. E*, 2002, **9**, 477.
57 N. Kikuchi, C. M. Pooley, J. F. Ryder and J. M. Yeomans, *J. Chem. Phys.*, 2003, **119**, 6388.
58 C. Campaña and M. H. Müser, *Phys. Rev. B: Condens. Matter Mater. Phys.*, 2006, **74**, 1781.
59 P. B. Canham, *J. Theor. Biol.*, 1970, **26**, 61.
60 E. A. Evans, *Biophys. J.*, 1973, **14**, 923.
61 W. Helfrich, *Z. Naturforsch., Teil C*, 1973, **28**, 693.
62 S. C. Brenner and R. L. Scott, *The Mathematical Theory of Finite Element Methods*, Springer, New York, 3rd edn, 2008.
63 P. R. Onck, T. Koeman, T. van Dillen and E. van der Giessen, *Phys. Rev. Lett.*, 2005, **95**.
64 J. A. Åström, S. P. Kumar, I. Vattulainen and M. Karttunen, *Phys. Rev. E: Stat., Nonlinear, Soft Matter Phys.*, 2008, **77**, 051913.
65 J. A. Åström, P. B. S. Kumar and M. Karttunen, *Soft Matter*, 2008, accepted.
66 F. Ziebert and I. S. Aranson, *Phys. Rev. E: Stat., Nonlinear, Soft Matter Phys.*, 2008, **77**.
67 H. Gohlke and M. F. Thorpe, *Biophys. J.*, 2006, **91**, 2115.
68 A. Arkhipov, P. L. Freddolino and K. Schulten, *Structure*, 2006, **14**, 1767.
69 Z. Zhang, L. Lu, W. G. Noid, V. Krishna, J. Pfaendtner and G. A. Voth, *Biophys. J.*, 2008, **95**, 5073.
70 D. Gfeller and P. D. L. Rios, *Phys. Rev. Lett.*, 2008, **100**, 174104.
71 R. L. Henderson, *Phys. Lett.*, 1974, **49A**, 197.
72 J. T. Chayes, L. Chayes and E. H. Lieb, *Commun. Math. Phys.*, 1984, **93**, 57.
73 J. T. Chayes and L. Chayes, *J. Stat. Phys.*, 1984, **36**, 471.
74 P. Hohenberg and W. Kohn, *Phys. Rev. B*, 1964, **136**, 864.
75 R. P. Feynman and H. Kleinert, *Phys. Rev. A*, 1986, **34**, 5080.
76 G. Tóth, *J. Phys.: Condens. Matter*, 2007, **19**, 335220.
77 A. P. Lyubartsev and A. Laaksonen, *Phys. Rev. E*, 1995, **52**, 3730.
78 R. Faller, H. Schmitz, O. Biermann and F. MŸller-Plathe, *J. Comput. Chem.*, 1999, **20**, 1009.
79 S. Girard and F. Müller-Plathe, *Mol. Simul.*, 2002, **101**, 779.
80 D. Reith, H. Meyer and F. Müller-Plathe, *Macromolecules*, 2001, **34**, 2235.
81 A. P. Lyubartsev and A. Laaksonen, *Chem. Phys. Lett.*, 2000, **325**, 15.
82 T. Murtola, E. Falck, M. Karttunen and I. Vattulainen, *J. Chem. Phys.*, 2007, **126**, 075101.
83 T. Murtola, E. Falck, M. Patra, M. Karttunen and I. Vattulainen, *J. Chem. Phys.*, 2004, **121**, 9156.
84 A. P. Lyubartsev, M. Karttunen, I. Vattulainen and A. Laaksonen, *Soft Mater.*, 2003, 121–137.
85 E. Falck, M. Patra, M. Karttunen, M. T. Hyvönen and I. Vattulainen, *Biophys. J.*, 2004, **87**, 1076.
86 T. Murtola, T. Róg, E. Falck, M. Karttunen and I. Vattulainen, *Phys. Rev. Lett.*, 2006, **97**, 238102.
87 F. Ercolessi and J. B. Adams, *Europhys. Lett.*, 1994, **26**, 583.
88 S. Izvekov, M. Parrinello, C. J. Burnham and G. A. Voth, *J. Chem. Phys.*, 2004, **120**, 10896.
89 S. Izvekov and G. A. Voth, *J. Chem. Phys.*, 2005, **123**, 134105.
90 S. Izvekov and G. A. Voth, *J. Phys. Chem. B*, 2005, **109**, 2469.
91 S. Izvekov and G. A. Voth, *J. Chem. Theory Comput.*, 2006, **2**, 637.
92 P. Liu, S. Izvekov and G. Voth, *J. Phys. Chem. B*, 2007, **111**, 11566.
93 J. Zhou, I. F. Thorpe, S. Izvekov and G. A. Voth, *Biophys. J.*, 2007, **92**, 4289.
94 Q. Shi, S. Izvekov and G. A. Voth, *J. Phys. Chem. B*, 2006, **110**, 1545.
95 W. G. Noid, J.-W. Chu, G. S. Ayton, V. Krishna, S. Izvekov, G. A. Voth, A. Das and H. C. Andersen, *J. Chem. Phys.*, 2008, **128**, 244114.
96 W. Noid, J.-W. Chu, G. Ayton and G. Voth, *J. Phys. Chem. B*, 2007, **111**, 4116.
97 A. A. Louis, *J. Phys.: Condens. Matter*, 2002, **14**, 9187.
98 S. J. Marrink, J. Risselada and A. E. Mark, *Chem. Phys. Lipids*, 2005, **135**, 223.
99 S. J. Marrink and A. E. Mark, *Biophys. J.*, 2004, **87**, 3894.
100 E. R. May, D. I. Kopelevich and A. Narang, *Biophys. J.*, 2008, **94**, 878.
101 S. Baoukina, L. Monticelli, M. Amrein and D. P. Tieleman, *Biophys. J.*, 2007, **93**, 3775.
102 M. L. Teodoro, J. Phillips, N. George and L. E. Kavraki, *J. Comput. Biol.*, 2003, **10**, 617.
103 P. Das, M. Moll, H. Stamati, L. E. Kavraki and C. Clementi, *Proc. Natl. Acad. Sci. U. S. A.*, 2006, **103**, 9885.
104 E. Plaku, H. Stamati, C. Clementi and L. E. Kavraki, *Proteins: Struct., Funct., Genet.*, 2007, **67**, 897.
105 S. Mesenteand, S. Fischer and J. C. Smith, *Proteins: Struct., Funct., Genet.*, 2006, **64**, 210.
106 S. T. Roweis and L. K. Saul, *Science*, 2000, **290**, 2323.
107 M. Belkin and P. Niyogi, *Neural Comput.*, 2003, **15**, 1373.
108 R. R. Coifman and S. Lafon, *Appl. Comput. Harmon. Anal.*, 2006, **21**, 5.
109 B. Nadler, S. Lafon, R. R. Coifman and I. G. Kevrekidis, *Appl. Comput. Harmon. Anal.*, 2006, **21**, 113.
110 P. S. Shenkin and D. Q. McDonald, *J. Comput. Chem.*, 1994, **15**, 899.
111 F. A. Hamprecht, C. Peter, X. Daura, W. Thiel and W. F. van Gunsteren, *J. Chem. Phys.*, 2001, **114**, 2079.
112 T. Kohonen, *Self-Organizing Maps, Vol. 30 of Springer Series in Information Science*, Springer, Berlin, 3rd edn, 2001.
113 S. Haykin, *Neural Networks—A Comprehensive Foundation*, Prentice-Hall, New Jersey, 1999.
114 T. Murtola, M. Kupiainen, E. Falck and I. Vattulainen, *J. Chem. Phys.*, 2007, **126**, 054707.
115 J. Vesanto, J. Himberg, E. Alhoniemi and J. Parhankangas, in *Proceedings of the Matlab DSP Conference 1999*, Espoo, Finland, 1999, pp. 35–40.
116 J. Schuchhardt, G. Schneider, J. Reichelt, D. Schomburg and P. Wrede, *Protein Eng., Des. Sel.*, 1996, **9**, 833.
117 M. T. Hyvönen, Y. Hiltunen, W. El-Deredy, T. Ojala, J. Vaara, P. T. Kovanen and M. Ala-Korpela, *J. Am. Chem. Soc.*, 2001, **123**, 810.
118 M. A. Andrade, G. Casari, C. Sander and A. Valencia, *Biochemistry*, 1997, **76**, 441.
119 S. Mahony, D. Hendrix, T. J. Smith and A. Golden, *Artif. Intell. Rev.*, 2005, **24**, 397.
120 S. Mahony, D. Hendrix, A. Golden, T. J. Smith and D. S. Rokhsar, *Bioinformatics*, 2005, **21**, 1807.
121 Z. R. Yang and K. C. Chou, *J. Chem. Inf. Comput. Sci.*, 2003, **43**, 1748.
122 J. T. Ayers, A. Clauset, J. D. Schmitt, L. P. Dwoskin and P. A. Crooks, *Am. Assoc. Pharm. Sci. J.*, 2005, **25**, E678.
123 J. Vesanto and E. Alhoniemi, *IEEE Trans. Neural Netw.*, 2000, **11**, 586.
124 W. G. Hoover, *Phys. Rev. A*, 1985, **31**, 1695.
125 S. Nosé, *J. Chem. Phys.*, 1984, **81**, 511.
126 S. Nosé, *Mol. Phys.*, 1984, **52**, 255.
127 H. J. C. Berendsen, J. P. M. Postma, W. F. van Gunsteren, A. DiNola and J. R. Haak, *J. Chem. Phys.*, 1984, **81**, 3684.
128 H. C. Andersen, *J. Chem. Phys.*, 1980, **72**, 2384.

129 R. D. Groot and P. B. Warren, *J. Chem. Phys.*, 1997, **107**, 4423.
130 T. Soddemann, B. Dünweg and K. Kremer, *Phys. Rev. E: Stat., Nonlinear, Soft Matter Phys.*, 2003, **68**, 046702.
131 J. A. Backer, C. P. Lowe, H. C. J. Hoefsloot and P. D. Ledema, *J. Chem. Phys.*, 2005, 154503.
132 J. G. E. M. Fraaije, B. A. C. van Vlimmeren, N. M. Maurits, M. Postma, O. A. Evers, C. Hoffmann, P. Altevogt and G. Goldbeck-Wood, *J. Chem. Phys.*, 1997, **106**, 4260.
133 U. Aaltosalmi, *PhD thesis*, Department of Physics, University of Jyväskylä, 2005.
134 G. Gonnella, E. Orlandini and J. M. Yeomans, *Phys. Rev. E*, 1998, **58**, 480.
135 M. Serrano, *Physica A*, 2006, **362**, 204.
136 P. J. Hoogerbrugge and J. M. V. A. Koelman, *Europhys. Lett.*, 1992, **19**, 155.
137 P. Español and P. Warren, *Europhys. Lett.*, 1995, **30**, 191.
138 P. Español, *Phys. Rev. E*, 1995, **52**, 1734.
139 R. D. Groot and K. L. Rabone, *Biophys. J.*, 2001, **81**, 725.
140 C. M. Wijmans, B. Smit and R. D. Groot, *J. Chem. Phys.*, 2001, **114**, 7644.
141 J. Shillcock and R. Lipowsky, *J. Phys.: Condens. Matter*, 2006, **18**, S1191.
142 A. G. Schlijper, P. J. Hoogerbrugge and C. W. Manke, *J. Rheol.*, 1995, **39**, 567.
143 N. A. Spenley, *Europhys. Lett.*, 2000, **49**, 534.
144 G. Pan and C. W. Manke, *Int. J. Mod. Phys. B*, 2003, **17**, 231.
145 P. Nikunen, I. Vattulainen and M. Karttunen, *Phys. Rev. E: Stat., Nonlinear, Soft Matter Phys.*, 2007, **75**, 036713.
146 K. Zhang and C. W. Manke, *Comput. Phys. Commun.*, 2000, **129**, 275.
147 Y. Kong, C. W. Manke, W. G. Madden and A. G. Schlijper, *Tribology Lett.*, 1997, **3**, 133.
148 A. G. Schlijper, C. W. Manke, W. G. Madden and Y. Kong, *Int. J. Mod. Phys. C*, 1997, **8**, 919.
149 J. S. Sims and N. Martys, *J. Res. Natl. Inst. Stand. Technol.*, 2004, **109**, 267.
150 R. D. Groot and T. J. Madden, *J. Chem. Phys.*, 1998, **108**, 8713.
151 R. D. Groot, T. J. Madden and D. J. Tildesley, *J. Chem. Phys.*, 1999, **110**, 9739.
152 L. Rekvig, M. Kranenburg, J. Vreede, B. Hafskjøld and B. Smit, *Langmuir*, 2003, **19**, 8195.
153 R. D. Groot, *Langmuir*, 2000, **16**, 7493.
154 M. Laradji and M. J. A. Hore, *J. Chem. Phys.*, 2004, **121**, 0641.
155 J. C. Shillcock and R. Lipowsky, in *NIC Symposium 2001, Proceedings*, ed. G. Rollnik and D. Wolf, John von Neumann Institute for Computing, Jülich, 2002, vol. 9 of *NIC Series*, pp. 407–417.
156 J. C. Shillcock and R. Lipowsky, *Nat. Mater.*, 2005, **4**, 225.
157 J. C. Shillcock and R. Lipowsky, *J. Phys.: Condens. Matter*, 2006, **18**, S1191.
158 S. Yamamoto and S.-A. Hyodo, *J. Chem. Phys.*, 2003, **118**, 7937.
159 A. F. Jakobsen, *J. Chem. Phys.*, 2005, **122**, 124901.
160 A. Kolb and B. Dünweg, *J. Chem. Phys.*, 1999, **111**, 4453.
161 C. Pastorino, T. Kreer, M. Müller and K. Binder, *Phys. Rev. E: Stat., Nonlinear, Soft Matter Phys.*, 2007, **76**, 026706.
162 C. P. Lowe, *Europhys. Lett.*, 1999, **47**, 145.
163 S. D. Stoyanov and R. D. Groot, *J. Chem. Phys.*, 2005, **122**, 114112.
164 M. P. Allen, *J. Phys. Chem. B*, 2006, **110**, 3823.
165 S. J. Marrink, D. P. Tieleman and A. E. Mark, *J. Phys. Chem. B*, 2000, **104**, 12165.
166 C. D. Bruce, S. Senapati, M. L. Berkowitz, L. Perera and M. D. E. Forbes, *J. Phys. Chem. B*, 2002, **106**, 10902.
167 A. R. Rakitin and G. R. Pack, *J. Phys. Chem. B*, 2004, **108**, 2712.
168 M. Sammalkorpi, M. Karttunen and M. Haataja, *J. Phys. Chem. B*, 2007, **111**, 11722.
169 M. Sammalkorpi, M. Karttunen and M. Haataja, *J. Am. Chem. Soc.*, 2008, **130**, 17977.
170 S. J. Marrink and A. E. Mark, *J. Am. Chem. Soc.*, 2003, **125**.
171 J. Feng, H. Liu, Y. Hu and J. Jiang, *Macromol. Theory Simul.*, 2008, **17**, 163.
172 F. Goujon, P. Malfreyt and D. J. Tildesley, *J. Chem. Phys.*, 2008, **129**, 034902.
173 C.-I. Huang, L.-F. Yang, C.-H. Lin and H.-T. Yu, *Macromol. Theory Simul.*, 2008, **17**, 198.
174 J. Huang, M. Luo and Y. Wang, *J. Phys. Chem.*, 2008, **112**, 6735.
175 O. Liba, D. Kauzlari, Z. R. Abrams, Y. Hanein, A. Greiner and J. G. Korvink, *Mol. Simul.*, 2008, **34**, 737.
176 J.-W. van de Meent, A. Morozov, E. Somfai, E. Sultan and W. van Saarloos, *Phys. Rev. E: Stat., Nonlinear, Soft Matter Phys.*, 2008, **78**, 015701.
177 H. Noguchi and G. Gompper, *Phys. Rev. E: Stat., Nonlinear, Soft Matter Phys.*, 2008, **78**, 016706.
178 C. Soto-Figueroa, M. del Rosario Rodriguez-Hidalgo, J.-M. Martinez-Magada and L. Vicente, *Macromolecules*, 2008, **41**, 3297.
179 A. Tiwari, H. Reddy, S. Mukhopadhyay and J. Abraham, *Phys. Rev. E: Stat., Nonlinear, Soft Matter Phys.*, 2008, **78**, 016305.
180 Y. Xu, J. Feng, H. Liu and Y. Hu, *Mol. Simul.*, 2008, **34**, 559.
181 A. Eriksson, M. N. Jacobi, J. Nyström and K. Tunström, *Phys. Rev. E: Stat., Nonlinear, Soft Matter Phys.*, 2008, **77**.
182 A. Eriksson, M. N. Jacobi, J. Nyström and K. Tunström, *J. Chem. Phys.*, 2008, **129**.
183 B. Dünweg and W. Paul, *Int. J. Mod. Phys. C*, 1991, **2**, 817.
184 L.-J. Chen, Z.-Y. Lu, H.-J. Qian, Z.-S. Li and C.-C. Sun, *J. Chem. Phys.*, 2005, **122**, 104907.
185 W. K. den Otter and J. H. R. Clarke, *Europhys. Lett.*, 2001, **53**, 426.
186 T. Shardlow, *SIAM J. Sci. Comput.*, 2003, **24**, 1267.
187 G. Besold, I. Vattulainen, M. Karttunen and J. M. Polson, *Phys. Rev. E*, 2000, **62**, R7611.
188 I. Pagonabarraga, M. H. J. Hagen and D. Frenkel, *Europhys. Lett.*, 1998, **42**, 377.
189 P. Nikunen, M. Karttunen and I. Vattulainen, *Comput. Phys. Commun.*, 2003, **153**, 407.
190 M. Serrano, G. De Fabritiis, P. Espanol and P. V. Coveney, *Math. Comput. Simul.*, 2006, **72**, 190.
191 E. A. Koopman and C. P. Lowe, *J. Chem. Phys.*, 2006, **124**.
192 A. F. Jakobsen, G. Besold and O. G. Mouritsen, *J. Chem. Phys.*, 2006, **124**, 094104.
193 A. F. Jakobsen, *J. Chem. Phys.*, 2006, **122**, 124901 125, 01029901.
194 M. Venturoli, M. M. Sperotto, M. Kranenburg and B. Smit, *Phys. Rep.*, 2006, **437**, 1.
195 C. Junghans, M. Praprotnik and K. Kremer, *Soft Matter*, 2008, **4**, 156.
196 E. G. Flekkøy, P. V. Coveney and G. De Fabritiis, *Phys. Rev. E*, 2000, **62**, 2140.
197 E. G. Flekkøy and P. V. Coveney, *Phys. Rev. Lett.*, 1999, **83**, 1775.
198 E. Lindahl and O. Edholm, *Biophys. J.*, 2000, **79**, 426.
199 M. Deserno, in *Computer Simulation Studies in Condensed Matter Physics XIX*, ed. D. P. Landau, S. P. Lewis and H. B. Schüttler, Springer, Heidelberg, 2006.
200 J.-M. Drouffe, A. C. Maggs and S. Leibler, *Science*, 1991, **256**, 1353.
201 H. Noguchi and M. Takasu, *Phys. Rev. E: Stat., Nonlinear, Soft Matter Phys.*, 2001, **64**, 041913.
202 H. Noguchi and M. Takasu, *J. Chem. Phys.*, 2001, **115**, 9547.
203 Z.-J. Wang and D. Frenkel, *J. Chem. Phys.*, 2005, **122**, 234711.
204 G. Brannigan and F. L. H. Brown, *J. Chem. Phys.*, 2004, **120**, 1059.
205 O. Farago, *J. Chem. Phys.*, 2003, **119**, 596.
206 G. Brannigan, P. F. Philips and F. L. H. Brown, *Phys. Rev. E: Stat., Nonlinear, Soft Matter Phys.*, 2005, **72**, 011915.
207 I. Cooke, K. Kremer and M. Deserno, *Phys. Rev. E: Stat., Nonlinear, Soft Matter Phys.*, 2005, **72**, 011506.
208 G. Brannigan and F. L. H. Brown, *Biophys. J.*, 2006, **90**, 1501.
209 O. Farago, *J. Chem. Phys.*, 2008, **128**, 184105.
210 V. A. Harmandaris and M. Deserno, *J. Chem. Phys.*, 2006, **125**, 204905.
211 H. J. Limbach, A. Arnold, B. A. Mann and C. Holm, *Comput. Phys. Commun.*, 2006, **174**, 704.
212 A. Arkhipov, Y. Yin and K. Schulten, *Biophys. J.*, 2008, **95**, 2806.
213 O. Farago, N. Grønbech-Jensen and P. Pincus, *Phys. Rev. Lett.*, 2006, **96**, 018102.
214 O. Farago, K. Ewert, A. Ahmad, H. M. Evans, N. Gronbech-Jensen and C. R. Safinya, *Biophys. J.*, 2008, **95**, 836.

215 B. J. Reynwar, G. Illya, V. A. Harmandaris, M. M. Müller, K. Kremer and M. Deserno, *Nature*, 2007, **447**, 461.
216 P. D. Blood and G. Voth, *Proc. Natl. Acad. Sci. U. S. A.*, 2006, **103**, 15068.
217 G. S. Ayton, P. D. Blood and G. A. Voth, *Biophys. J.*, 2007, **92**, 3595.
218 R. D. Groot, *J. Chem. Phys.*, 2003, **118**, 11265.
219 R. D. Groot, *J. Chem. Phys.*, 2003, **119**.
220 S. Izvekov, J. M. J. Swanson and G. A. Voth, *J. Phys. Chem. B*, 2008.
221 M. Karttunen, J. Rottler, I. Vattulainen and C. Sagui, in *Electrostatics in Biomolecular Simulations Where Are We Now and Where Are We Heading?*, ed. S. Feller, Elsevier, Amsterdam, 2008, vol. 60, pp. 49–89.
222 J. Fan, M. Sammalkorpi and M. Haataja, *Phys. Rev. Lett.*, 2008, **100**.
223 L. Kale and S. Kirshnan, in *Parallel Programming using C++*, ed. G. Wilson and P. Lu, MIT Press, Boston, 1996, pp. 175–213.
224 J. E. E. Stone, J. C. C. Phillips, P. L. L. Freddolino, D. J. J. Hardy, L. G. G. Trabuco and K. Schulten, *J. Comput. Chem.*, 2007, **28**, 1618.
225 J. A. van Meel, A. Arnold, D. Frenkel, Portegies and R. G. Belleman, *Mol. Simul.*, 2008, **34**, 259.
226 S. J. Plimpton, *J. Comput. Phys.*, 1995, **117**, 1.
227 D. Van Der Spoel, E. Lindahl, B. Hess, G. Groenhof, A. E. Mark and H. J. Berendsen, *J. Comput. Chem.*, 2005, **26**, 1701.
228 L. Kalé, R. Skeel, M. Bhandarkar, R. Brunner, A. Gursoy, N. Krawetz, J. Phillips, A. Shinozaki, K. Varadarajan and K. Schulten, *J. Comput. Phys.*, 1999, **151**, 283.
229 J. C. Phillips, R. Braun, W. Wang, J. Gumbart, E. Tajkhorshid, E. Villa, C. Chipot, R. D. Skeel, L. Kale and K. Schulten, *J. Comput. Chem.*, 2005, **26**, 1781.
230 W. Humphrey, A. Dalke and K. Schulten, *J. Mol. Graphics*, 1996, **14**, 33.
231 A. P. Lyubartsev and A. Laaksonen, *Comput. Phys. Commun.*, 2000, **128**, 565.
232 M. Doi, *J. Comput. Appl. Math.*, 2002, **149**, 13.

